Journal Pre-proofs

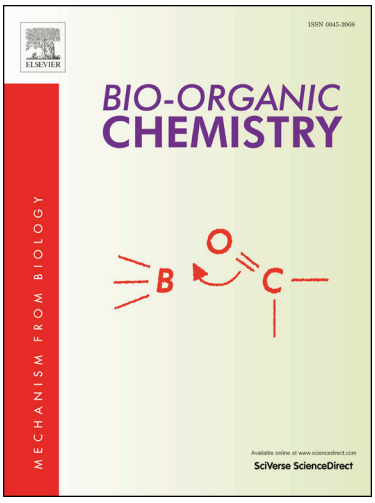

Assessment of elementary derivatives of 1,5-benzodiazepine as anticancer agents with synergy potential

Sinthiya J. Gawandi, Vidya G Desai, Shrinivas Joshi, Sunil Shingade, Raghuvir Pissurlekar

PII: S0045-2068(21)00708-2
DOI: https://doi.org/10.1016/j.bioorg.2021.105331
Reference: YBIOO 105331

To appear in: *Bioorganic Chemistry*

Received Date: 16 April 2021
Revised Date: 26 August 2021
Accepted Date: 1 September 2021

Please cite this article as: S.J. Gawandi, V.G. Desai, S. Joshi, S. Shingade, R. Pissurlekar, Assessment of elementary derivatives of 1,5-benzodiazepine as anticancer agents with synergy potential, *Bioorganic Chemistry* (2021), doi: https://doi.org/10.1016/j.bioorg.2021.105331

Graphical Abstract

Assessment of elementary derivatives of 1,5-benzodiazepine as anticancer agents with synergy potential

Sinthiya J Gawandi , Vidya G Desai *, Shrinivas Joshi , Sunil Shingade and Raghuvir Pissurlekar

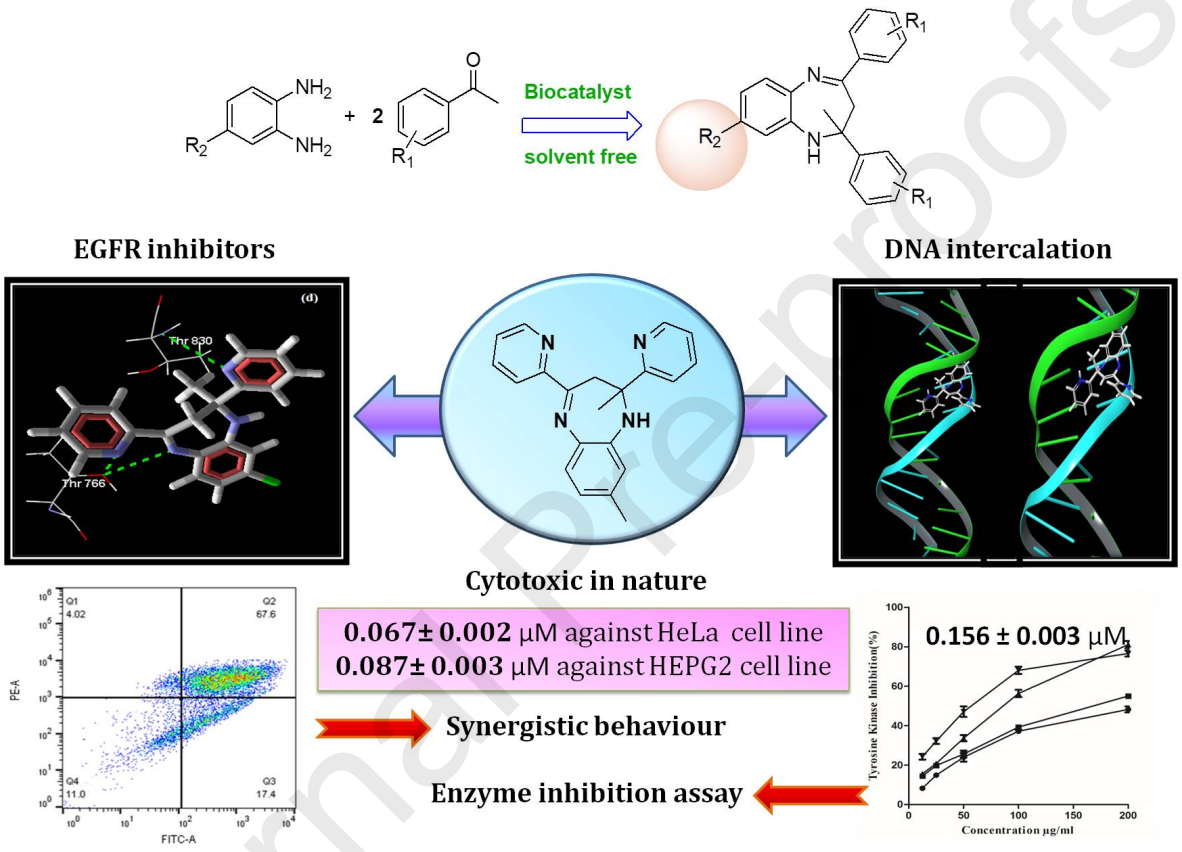

Assessment of elementary derivatives of 1,5-benzodiazepine as anticancer agents with synergy potential

Sinthiya J Gawandi[a] , Vidya G Desai[a] ∗, Shrinivas Joshi[b] , Sunil Shingade[c] and Raghuvir Pissurlekar[d]

[a] *Department of Chemistry, Dnyanprassarak Mandal's College & Research Centre, Assagao, Bardez 403507, India.*

[b] *Novel Drug Design and Discovery Laboratory, Department of Pharmaceutical Chemistry, S.E.T.'s College of Pharmacy, Sangolli Rayanna Nagar, Dharwad, 580 002, Karnataka, India.*

[c]*SSPM's V P College of Pharmacy, Madkhol, Sawantwadi, Sindhudurg, Maharashtra.*

[d]*(Bio) Molecular Simulations Group, Department of Pharmaceutical Chemistry, Goa College of Pharmacy, Panaji Goa, India.*

Dedicated to my Ph.D. mentor Professor Santosh G. Tilve on his 62nd birthday

Abstract:

Herein, we designed and synthesized 1,5-benzodiazepines as a lead molecule for anticancer activity and as potent synergistic activity with drug Methotrexate. Working under the framework of green chemistry principles, series of 1,5-benzodiazepine derivatives **(3a-3a[1])** were synthesized using biocatalyst i.e. thiamine hydrochloride under solvent free neat heat conditions. These compounds were screened for *in vitro* anti cancer activity against couple of cancer cell lines (HeLa and HEPG2) and normal human cell line HEK-293 via MTT assay. The IC_{50} values for the compounds were in the range 0.067 to 0.35 μM, better than Paclitaxel and compatible with the drug Methotrexate. Compound **3x** was found to be influential against both the cell lines with IC_{50} values of 0.067± 0.002 μM against HeLa and 0.087± 0.003 μM against HEPG2 cell line, having activity as compatible to the standard drug Methotrexate. Bioinformatic analysis showed that these compounds are good tyrosine kinase inhibitors which was then proved using enzyme inhibition assay. The studies of apoptosis revealed late apoptotic mode of cell death for the compounds against HEPG2 cancer cell line using flow cytometry method. Synergistic studies of compound **3x** and drug Methotrexate showed that the combination was highly active against cancer HeLa and HEPG2 cell line with IC50 value 0.046 ± 0.002 μM and 0.057 ± 0.002 μM respectively, which was well supported by apoptosis pathway. Further the compounds proved its scope as DNA intercalating agents, as its molecular docking and DNA binding studies revealed that the compounds would fit well into the DNA strands.

Keywords:

1,5-benzodiazepines, thiamine hydrochloride, cytotoxicity, apoptosis, molecular docking.

Corresponding Author:

Tel.: 9822180792; fax: 0832-2268683; e-mail: desai_vidya@ymail.com

1. Introduction:

Cancer is one of the topmost malignant diseases responsible for millions of demise of people per year worldwide. Principally, numbers of deaths arise from leukemia, breast, cervical and liver cancer. There is a continuous struggle for the advancement of new drug therapies for safe and effective treatment of cancer disease[1,2,3]. One of the therapies that have proven it has been the drug combination therapy[4,5,6]. Combinations of two or more drugs can conquer over toxicity and other side effects linked with steep shot of single drugs by resisting biological compensation, thereby treating multifactorial disease. Synergistic drug combination studies have gained a promising research strategy with the motif of enhancing drug effect; improve drug selectivity by overcoming unwanted side effects, host immunity and lowering normal cell toxicity current drug therapeutics by development of novel drug treatment strategies. Administering more than one drug can provide several benefits that include better efficacy, lower toxicity, and much delay in onset of acquired drug resistance[7,8,9]

In cancer drug discovery, Tyrosine kinase is the key enzyme in the sub group of protein kinases, responsible for phosphate group transfer from ATP to a protein in a cell which is a vital mechanism in signal transduction and cell regulation[10,11,12]. Epidermal growth factor receptor (EGFR)-TK is found to be over expressed in most of the solid tumors. It leads to autophosphorylation of protein, thus triggering the tumor growth and expansion leading to malignant progression[13, 14]. The most common drugs known for inhibition of these enzymes are Gefitinib[15], Imatinib[16], Erlotinib[17], etc. (Fig 1)

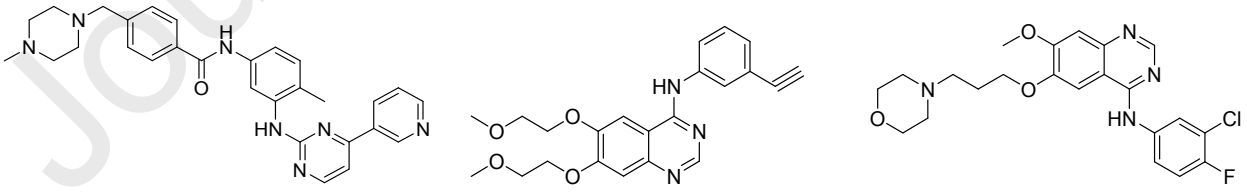

Imatinib **Erlotinib** **Gefitinib**

Fig 1: Drugs known as EGFR tyrosine kinase inhibitors

Kinase inhibitors as monotherapy have not been so effective for treating large cases of malignances and hence synergistic combination is an alternative to look forward to[18]. Simple compounds have been synergised with EGFR tyrosine inhibitors in an anticancer synergy[19, 20]. A potential combination therapy for the treatment of advanced ovarian cancer has been reported involving FDA-

approved targeted drugs—sunitinib, dasatinib, and everolimus[21]. In silico modelling methods have been used to predict synergism of cancer drug combinations[22].

The mechanism of action of main anticancer drugs like Cis-platin, Paclitaxel and Methotrexate takes place by inhibiting DNA synthesis and suppressing RNA transcription [23], stabilization of microtubule [24] and by inhibition of dihydrofolate reductase[25] respectively, can hold a great scope in combination therapy. (fig 2)

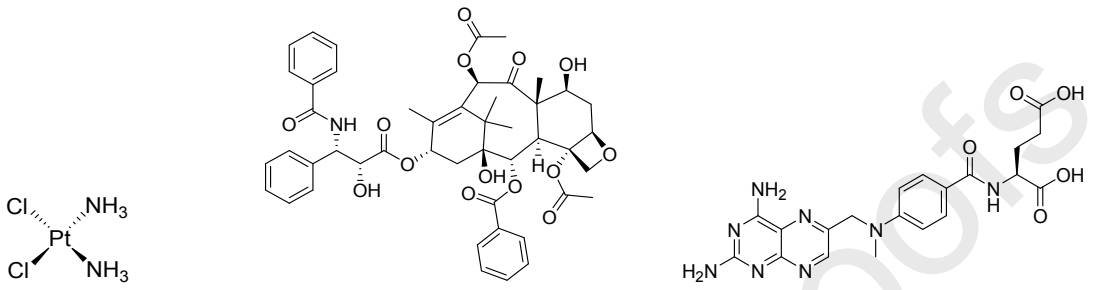

Cis-platin Paclitaxel Methotrexate

Fig 2. Standard drugs used as anticancer agents

Amongst these, Methotrexate is one such drug which acts by reducing the amount of tetrahydrofolate required for the synthesis of purine bases. This action results in death of cancer cells[26]. Being also a powerful medication for variety of autoimmue disorders such as psoriasis[27] and rheumatoid arthritis[28], it has been commonly used in synergy with variety of drugs that include 5-Fluorouracil[29], Infliximab[30], Cytarabine[31] etc. Despite efforts, developing an attractive experimentation on synergism for cancer drug development is indeed a challenging task.

Benzodiazepine a pharmacophoric scaffold containing a ring complex made up of a benzene ring and a diazepam ring represents a class of psychoactive drugs. Besides, enhancing the effect of gamma-aminobutyric acid at the GABA receptor resulting in the sedative, hypnotic and anti-depressant activity, benzodiazepines exhibit wide range other significant biological applications[32-38]. Moreover,benzodiazepines have attracted attention of chemist in the field of drugs and pharmaceuticals[39].

The most commonly employed synthetic protocol for 1,5-benzodiazepines includes coupling diamines with α,β-unsaturated ketone [40, 41], aliphatic ketones [42], β- diketones [43], β-ketoesters [44] in presence of acid or base. Distinct range of catalysts have been employed in the synthesis of 1,5-benzodiazepines [45-56]. Solvent free organic synthesis and transformations are said to be industrially constructive and green[57]. In our synthetic strategy towards 1,5-benzodiazepines, we choose Thiamine hydrochloride also called as vitamin B1, a water soluble vitamin employed as organocatalyst by virtue of its properties such as non- toxic, metal free, inexpensive, ease of isolation procedures etc. As a result of its structural appearance it has been considered as a powerful biocatalyst for various organic transformations by many synthetic organic chemists.[58-61] (Fig 3)

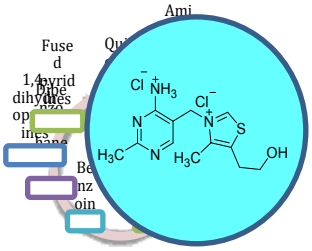

Fig 3: Thiamine Hydrochloride (Vitamin B1)

As an extension to our work towards the development of methodologies for the synthesis of heterocyclic compounds, we hereby report an efficient and ecofriendly method for the synthesis of 1,5-benzodiazepines from substituted o-phenylenediamine and ketones. A simple model substrate was examined to establish the viability of the approach and to optimize the reaction conditions in presence of a biocatalyst under solvent free conditions. In view of the recent developments towards metal free synthesis, we decided to explore thiamine hydrochloride as catalyst.

2. Results and Discussion

2.1. Chemistry

Derivatives of 2-Methyl-2,4-diphenyl-2,3-dihydro-1H-benzo[1,5]diazepine have been synthesized by condensation of substituted 2,3-diamino benzenes with different ketone substrates in presence of thiamine hydrochloride as a catalyst under solvent free neat heat conditions at 70-80°C. The synthesis of compounds **3a-3a**[1] has been carried out as outlined in (**scheme 1**). To synthesize compounds **3a-3e** the condensation was carried out between o-phenylene diamine and substituted ketones. Similarly, to obtain compound **3f - 3l** and **3m - 3s** 4-methyl-2-nitro-aniline and 4-chloro-2-nitro-aniline were initially reduced to 4-methyl-1,2-diamino benzene and 4-chloro-1,2 diamino benzene respectively using Sn/ HCl and were then condensed with ketone substrates using the same model methodology. The benzodiazepine derivatives **3t-3w** were synthesized by condensation of ketones with 4-bromo-1,2 diamino benzene.

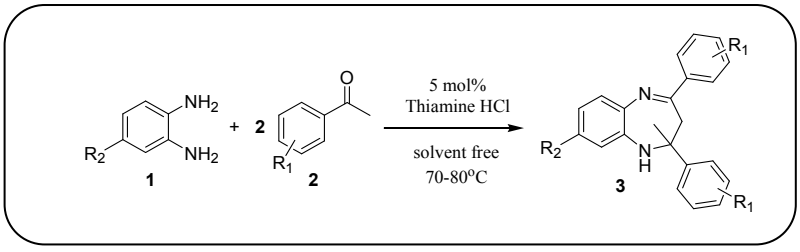

Scheme 1: Methodology for the synthesis of 1,5-benzodiazepines derivatives

In the initial experiment, optimization was carried out wherein; acetophenone substrate was used as a representative substrate. The efficiency of the reaction depends on the physical factors such as amount of catalyst, temperature of the reaction and the type of solvent used. The optimal reaction conditions were investigated by varying the temperature, catalyst and solvent of the reaction system. Ultimately, 5 mol% of

catalyst under solvent free neat heat reaction condition was witnessed as the most efficient method to carry out the synthesis. To study the synthetic utility of the employed catalyst and optimized reaction conditions, the methodology was applied on differently substituted o-phenylenediamine and ketone substrates. All the substituted aromatic and heterocyclic ketone substrates as well as substituted diamines reacted well to afford respective derivatives in good yields.

In all the cases, the reaction was monitored using thin layer chromatography. After completion, the reaction was quenched in water, followed by extraction in ethyl acetate. The crude product obtained was further isolated using column chromatography. The scope and generality of this method was extended by scrutinizing electronically divergent substituted ketones bearing various electron withdrawing or electron donating groups at ortho, meta, or para positions of the aromatic ring. Substitution pattern in target synthesis plays an important role in drug development. Presence of specific substituents such as halogens, alkyl and nitro, methoxy can be of great utility towards structure activity relationship studies. The results are encapsulated in Table 1**.** Para substituted nitro acetophenone was found to be most reactive for the condensation to take place with all the different substituted o-phenylenediamines. It was also inferred from the results that the yields of the product with respect to electron withdrawing substrates were higher in comparison to that of the electron donating substrates. Likewise, parent o-phenylene diamine showed better reactivity in terms of yields as compared to those of the substituted diamines

Table 1: List of synthesized 1,5-benzodiazepine derivatives detailing substrate scope for the reaction

Compound	***R_1***	***R_2***	***Time in h***	***% yield***	***Expt. M. Pt. ^oC***	***Lit M. Pt. ^oC***
3a	H	H	1	66	140-142	143-145
3b	4-Br	H	3	66	140-144	145-146
3c	4-Cl	H	4	72	138-144	140-142
3d	4-NO_2	H	3	75	146-148	148-150
3e	3-NO_2	H	3.5	68	156-160	158-160
3f	H	CH_3	4.5	27	148-150	148-150
3g	4-NO_2	CH_3	3.5	55	146-150	N.R
3h	4-Br	CH_3	4	55	156-160	N.R
3i	4-Cl	CH_3	2.5	49	138-142	N.R
3j	3-Br	CH_3	4	50	150-154	N.R
3k	3-NO_2	CH_3	3	52	134-136	N.R
3l	4-OMe	CH_3	3	52	78-80	N.R
3m	H	Cl	3.5	62	138-140	138-142
3n	4-NO_2	Cl	3	66	162-164	N.R
3o	4-Br	Cl	3	58	154-156	N.R
3p	4-Cl	Cl	3.5	54	146-148	N.R
3q	3-NO_2	Cl	3.5	57	138-140	N.R

3s	4-F	Cl	3.5	35	138-140	N.R
3t	4-NO_2	Br	2.5	62	162-164	N.R
3u	4-Cl	Br	3.5	56	172-174	N.R
3v	3,4-OMe	Br	3.5	45	122-124	N.R
3w	3- NO_2	Br	4	57	136-138	N. R

In order to investigate the feasibility of this synthetic methodology, towards differently substituted substrates and with a perspective of developing a better biologically active molecule, we synthesized scaffolds containing benzodiazepine. Pyridine being part of many natural products such as vitamins coenzymes is an interesting molecule with its beneficial drug favoring characteristics which includes its smaller size, basicity, water solubility, hydrogen bonding capability [62]. Naphthalene has also been seen as one of the most privileged molecule in the drug discovery field and has also been reported to possess anticancer properties[63, 64]. Thus, to study the effect of these moieties in combination with benzodiazepine molecule we designed few molecules and examined the alterations in the biological properties. The synthesis was accomplished through a condensation reaction between substituted 1,2-diaminobenzenes with 2-acetyl pyridine, 4-acetyl pyridine and 2- acetyl naphthalene compounds (scheme 2).

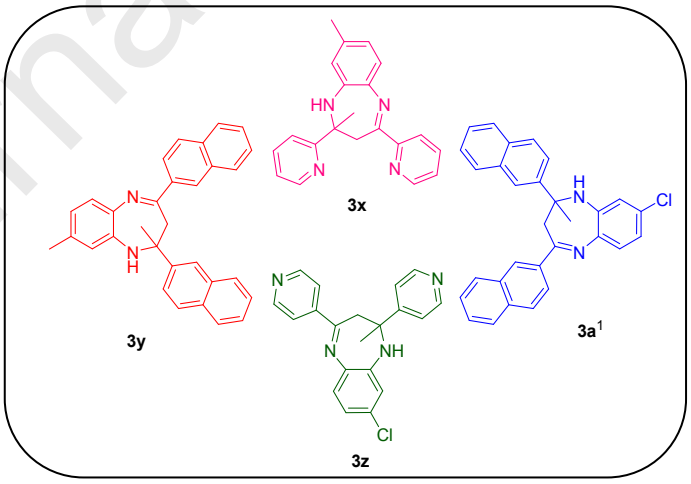

Scheme 2: Synthesis of scaffold containing 1,5-benzodiazepines

The newly synthesized compounds have been characterized by ^{1}H NMR, ^{13}C NMR and mass spectroscopy. 1H NMR analysis confirms the formation of 1,5 -benzodiazepine structure. The main distinctive peaks in the

signifying the CH_2 protons at C3 of the seven membered benzodiazepine ring. The most deshielded proton was observed in case of the aromatic hydrogen present on the phenyl ring substituted on C4 of the benzodiazepine ring. All the aromatic protons appeared as multiplets in the region δH 8.00 to 6.5ppm, thereby marking the formation of 1,5-benzodiazepine derivatives. Along with this, ^{13}C NMR spectroscopic study also signifies the benzodiazepine formation. In C13 NMR spectra of all the compounds the characteristic peak of C4 (C=N) of the benzodiazepine ring appeared in the range of 164.7-167.2 ppm. Signal due to C2 was observed in the range of 72.7-73.4 ppm. Characteristic peak of formation of benzodiazepine ring signifying C3 (methylene-CH_2) carbon appeared at 42.9- 43.4 ppm which was also confirmed in DEPT analysis. The exact molecular weight was also characterized and confirmed by HRMS studies. Purity of the compounds was checked using HPLC studies .

2.2. Biological activity

2.2.1. *In-vitro screening*

2.2.1.2. *Cytotoxicity assay*

In vitro cytotoxicity of the selected compounds **3a**, **3k**, **3q**, **3w**, **3y** and **3x** was determined by the MTT [(3-(4,5-dimethyl-2- thiazolyl) 2,5-diphenyl-2H-tetrazolium bromide)] assay against a panel of three different human cancer cell lines namely; HEPG2 (human liver carcinoma), HeLa (human cervical) and HEK-293T (Human embryonic kidney cells) normal cell line. The concentration required to suppress 50% of the tumor cells i.e. IC_{50} values of the screened compounds and the reference drugs, Paclitaxel and Methotrexate are outlined in **Table 2**. As noticed, all compounds showed significant antitumor activities with IC_{50} values in the range of 0.067-1.65 μM, this indicated that the 1,5-benzodiazepine group can intensify the antitumor effects. Compound **3x** bearing the 2,4-dipyridinyl group, on the benzodiazepine nucleus was found to be the most potent among all the screened compounds and showed enhanced activity (IC_{50} values 0.067 μM against HeLa cell line and 0.087 μM against HepG2 cell line) against both the cancer cell lines . This was followed by compound **3q** with 3'-nitro substituted phenyl group on benzodiazepine ring, which displayed 0.10 ± 0.004 μM against HeLa cell line and 0.16±0.01 μM against HepG2 cancer cell line. All the screened compounds **3a**, **3k**, **3q**, **3w**, **3x** and **3y** were found to show better activity (0.067-0.21 μM) against HeLa cell lines compared to one of the reference compound Paclitaxel (IC_{50} values 0.23 μM). Compound **3x** showed analogous activity with respect to the other reference compound Methotrexate (IC_{50} values 0.057 and 0.083 μM). Other screened compounds also showed good activity against both the cell lines. It is clear from the results that almost all the targets exhibit moderate to good cytotoxicity against human liver carcinoma and cervical cancer cell lines although very weakly toxic against normal human embryonic kidney cells. The cell viability action was observed in a dose-dependent manner. Impressively, the cell viability decreased with the increase in concentration of the compounds against the tabbed cancer cell lines. In case of compound **3x** the cell viability dropped off significantly to 65.7%, 48.3%, 38.4%, 34.7%, 29.2%, 24.9% with the concentrations of 12.5, 25, 50, 100, 200 and 400 μg/mL respectively. **figure 4**.

compounds

Compound	*R*	*R_1*	*HeLa[a]*	*HepG2[b]*	*HEK293[c]*	*SI[d]-HeLa*	*SI-HEPG2*
3a	H	H	0.13 ± 0.008	0.34±0.02	0.72±0.03	5.53	2.11
3k	3-NO_2	CH_3	0.15 ± 0.006	0.35±0.04	0.39±0.02	2.60	1.11
3q	3-NO_2	Cl	0.10 ± 0.004	0.16±0.01	1.65±0.03	16.50	16.5
3w	3-NO_2	Br	0.13 ± 0.007	0.16±0.02	0.53±0.01	4.07	10.31
3y	2-Naphthyl	CH_3	0.21 ± 0.01	0.22±0.03	0.61±0.04	2.90	2.90
3x	2-pyridinyl	CH_3	0.067 ± 0.002	0.087±0.003	0.31±0.02	4.62	3.56
Paclitaxel			0.23± 0.02	0.28±0.03	-	-	-
Methotrexate			0.057± 0.001	0.083± 0.002	0.44± 0.01	-	-

a: human cervical cancer cell line

b: human liver carcinoma cell line

c: human embryonic kidney cell line

d: selectivity index was calculated as ratio of IC_{50} value of normal human cell line to that of the cancerous cell line.

IC_{50} values are obtained as the mean ± SD (μM) from three different experiments.

On the basis of these results structure activity relationship studies were executed by understanding the effect of substituents on cytotoxicity of the compounds. Compound **3a** with no substitution on either of the rings displayed moderate activity. Replacement of phenyl ring with heterocylic ring i.e. 2-pyridinyl moiety resulted in highest activity whereas substitution with a non-heterocyclic moiety like naphthalene showed lowest activity among all the compounds. Considering the substitution on 2 and 3 position on benzodiazepine ring the order of cytotoxicity can be drawn as follows 2-pyridinyl > 4-NO_2-phenyl > H > 2-Naphthyl. Substitution variation on the phenyl ring of the benzodiazepine ring was also studied. Presence of electron withdrawing group such as Cl and Br showed good activity compared to the electron donating methyl group. Among the two halogens, the most electronegative Chlorine group showed better activity as compared to bromine group. With respect to phenyl ring substitution, the cytotoxicity order is Cl > Br > H > CH_3. The selectivity index (SI) value >2 proved better selectivity and lower cytotoxicity of the synthesized compounds.

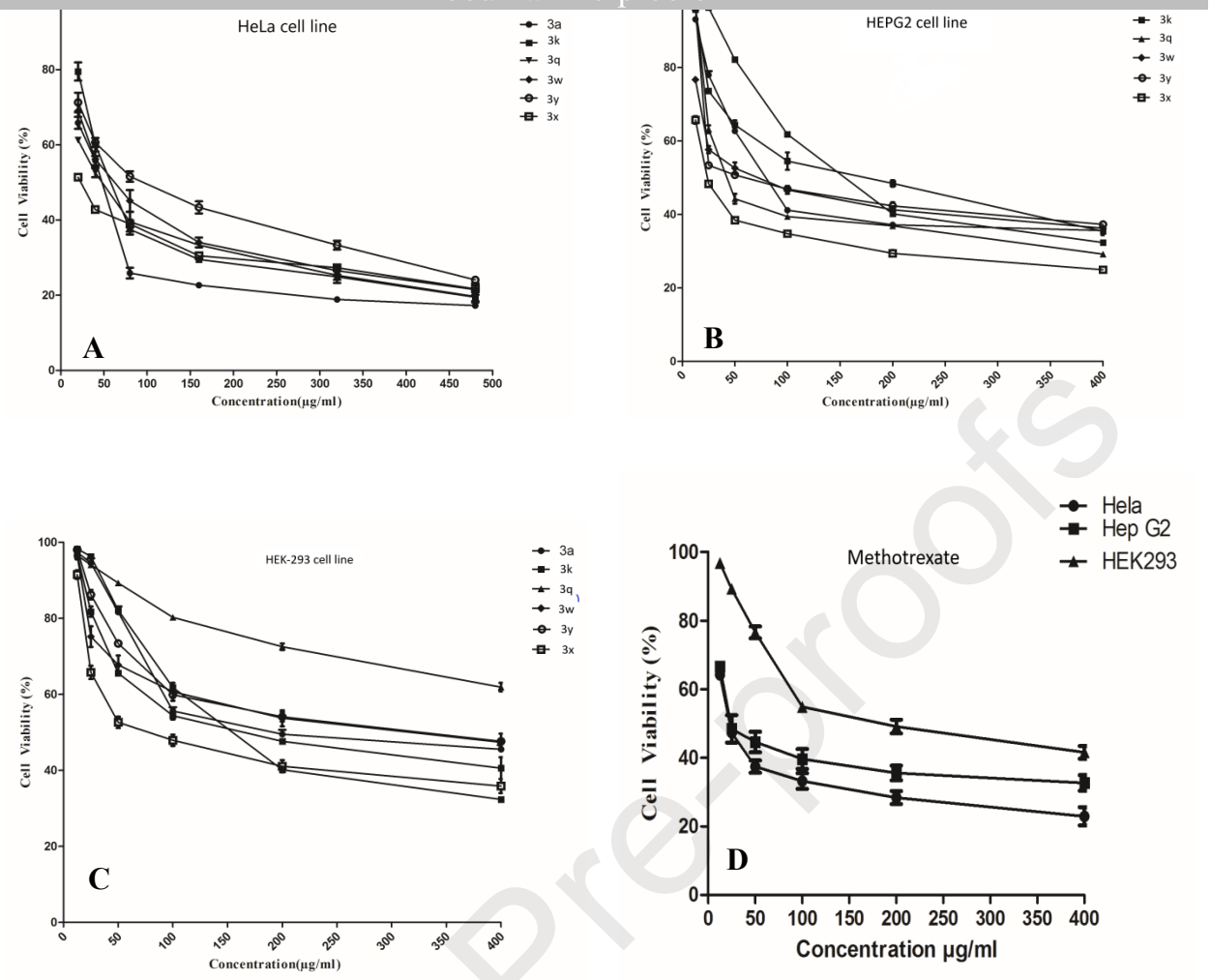

Figure 4: Dose- dependent effect on cell viability of selected compounds for three different cell lines a: for HeLa cell line, b: for HepG2 cell line c: for HEK-293 cell line, d: cell viability exhibited by methotrexate for all the three cell lines.

2.2.2.2. ***EGFR-Tyrosine kinase inhibition assay***

These potent molecules were aimed as EGFR- tyrosine kinase inhibitors. To study the strength of inhibitory activity and inhibition pathway, the inhibitory concentration IC_{50} values were determined against EGFR-tyrosine kinase enzyme using ELISA method. The IC_{50} values of the synthesized compounds against ranged from 0.156 to 0.514 µM (**Table 3**). Interestingly, among all the studied derivatives, compound **3x** displayed prominent inhibition with IC_{50} value 0.156 ± 0.003 µM. Structural divergences appeared to affect the potency of these compounds against the screened enzyme.

Table 3: IC_{50} values of *in vitro* tyrosine kinase inhibition assay

Compound	**Tyrosine Kinase Inhibition ($IC_{50\ in}$ µM)[a]**
3d	0.514 ± 0.003
3k	0.404 ± 0.002

3x	**0.156 ± 0.003**
Erlotinib	**0.08 ± 0.04**

a: Data are average of two independent runs

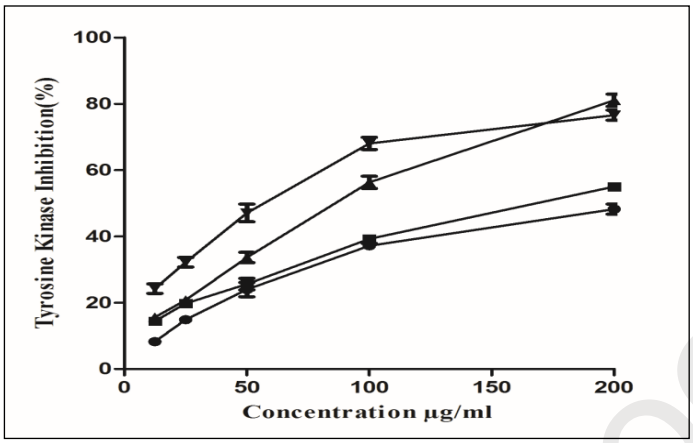

Figure 5: Graphical representation of tyrosine kinase inhibition activity

2.2.2.3. Annexin V- FITC/ Propidium iodide dual staining assay:

To investigate the mechanism underlying the antiproliferative effect of these potent compounds, the mode of tumor cell death was analyzed by fluorescence activated cell sortor (FACS) caliber on HepG2 liver cancer cells treated with 20µM of selected compounds for 24 h. The most prevailing technique used to study cell apoptosis/ necrosis is flow cytometry using propidium iodide (PI) and annexin V-FITC as dyes to spot viable and dead cells. A negative control was used for the analysis. This assay facilitate the detection of live cells (Q1-LL; AV-/PI-), early apoptotic cells (Q1-LR; AV+/PI-), late apoptotic cells (Q1-UR; AV+/PI+) and necrotic cells (Q1-UL; AV-/PI+). As shown in **figure 6**, flow cytometry analysis revealed that HepG2 cells treated with compounds **3q**, **3w**, **3y** and **3x** showed apoptosis. The percentage of late apoptotic cells induced by compound **3q**, **3w**, **3y** and **3x** was 10.2%, 13.0%, 5.54% and 64.6% respectively.

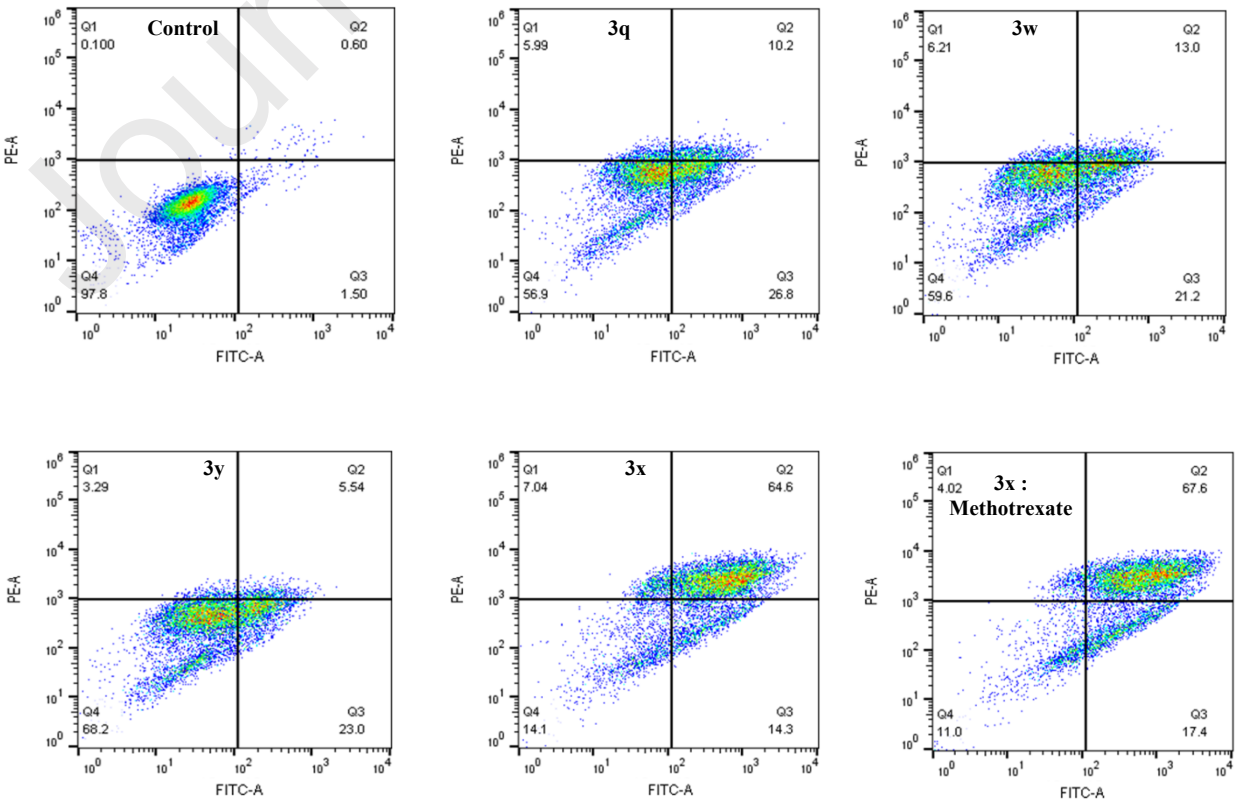

Figure 6. The apoptosis of HepG-2 cells was detected by flow cytometry. HepG-2 cells were pre-treated without the addition of any samples, the control (C) (I); with a dose of 20 μM of compounds for 24 h. Cells were stained with Annexin-V and PI. The evaluation of apoptosis is via Annexin V: FITC Apoptosis Detection Kit per manufacture's protocol. And the quantitative results were shown in (V). In each scatter diagrams, the abscissa represents the fluorescence intensity of the cells dyed by Annexin V; and the ordinate represents the fluorescence intensity of the cells dyed by PI. The percentage of cells positive for Annexin V-FITC and/or Propidium iodide is represented inside the quadrants. Cells in the upper left quadrant (Q1-UL; AV-/PI+): necrotic cells; lower left quadrant (Q1-LL; AV-/PI-): live cells; lower right quadrant (Q1-LR; AV+/PI-): early apoptotic cells and upper right quadrant (Q1-UR; AV+/PI +): late apoptotic cells.

2.2.2.4. **Synergistic activity of compound 3x with drug methotrexate:**

Synergistic drug combination studies have gained a promising research strategy with the motif of enhancing drug effect; improve drug selectivity by overcoming unwanted side effects, host immunity and lowering normal cell toxicity current drug therapeutics by development of novel drug treatment strategies. Synergistic combinations of two or more drugs can conquer over toxicity and other side effects linked with steep shot of single drugs by resisting biological compensation, thereby treating multifactorial diseases. Striving to implement this strategy using our synthesized compound, we combined it with the methotrexate drug which is widely known as anti cancer agent. Synergistic studies were carried out against HeLa and HEPG2 cancer cell lines using combination of compound **3x** and drug Methotrexate. As can be seen in **Table 4**, the results showed very good activity higher than the individual IC_{50} values against both the tested cancer cell lines. The combination resulted in improved activity with IC_{50} values of 0.046 ± 0.002 against HeLa cell line and 0.057 ± 0.002 against HEPG2 cell line. Enhancement in activity was also observed in case of flow cytometric analysis for cell death mode studies. The percentage of late apoptotic cells induced by the combination was 67.6% as shown in **figure 6**.

Table 4 : Synergistic activity of compound **3x** with Methotrexate for cytotoxicity studies

Compound	R	R_1	HeLa[a]	HEPG2[b]	HEK293[c]	SI[d]-HeLa	SI-HEPG2
3x	2-pyridinyl	CH_3	0.067 ± 0.002	0.087±0.003	0.31±0.02	4.62	3.56
3x :Methotrexate	-	-	0.046 ± 0.002	0.057 ± 0.002	-	-	-
Methotrexate			0.057± 0.001	0.083± 0.002	0.44± 0.01	-	-

a: human cervical cancer cell line b: human liver carcinoma cell line c: human embryonic kidney cell line

d: selectivity index was calculated as ratio of IC_{50} value of normal human cell line to that of the cancerous cell line. IC_{50} values are obtained as the mean ± SD (μM) from three different experiments

2.2.3.1. As dihydrofolate reductase inhibitors (anticancer agents)

To investigate the mechanism of antitumor activity and detailed intermolecular interactions between the synthesized compounds, molecular docking studies were performed on the crystal structure of dihydrofolate reductase complexed with NADPH and Methotrexate using the surflex-dock programme of sybyl-X 2.0 software. All the inhibitors were docked into the active site of enzyme as shown in **Figure 7** (A and B). The docking study revealed that all the compounds have showed very good docking score as dihydrofolate reductase inhibitors.

As depicted in the **figure 8**(A and B), compound **3q** makes five hydrogen bonding interactions at the active site of the enzyme (PDB ID: 1DF7), among those three interactions were of oxygen atom of nitro group present at 3rd position of phenyl ring with hydrogen atoms of ARG60 and ARG32 (O----H-ARG60, 2.20 Å, 2.57Å; O----H-ARG32, 2.14 Å), another oxygen atom of nitro group present at 3rd position of phenyl ring makes hydrogen bonding interaction with hydrogen atom of ARG32 (O----H-ARG60, 2.14 Å) and nitrogen atom of nitro group present at 3rd position of phenyl ring makes hydrogen bonding interaction with hydrogen atom of ARG60 (N----H-ARG60, 2.49 Å).

As depicted in the **figure 9**(A and B), compound **3w** makes six hydrogen bonding interactions at the active site of the enzyme (PDB ID: 1DF7), among those three interactions were of oxygen atom of nitro group present at 3rd position of phenyl ring with hydrogen atoms of ARG60 and ARG32 (O----H-ARG60, 2.60 Å, 2.25Å; O----H-ARG32, 2.18 Å), another oxygen atom of nitro group present at 3rd position of phenyl ring makes hydrogen bonding interactions with hydrogen atoms of ARG32 and TYR100 (O----H-ARG60, 1.71 Å; O----H-TYR100, 2.55 Å) and nitrogen atom of nitro group present at 3rd position of phenyl ring makes hydrogen bonding interaction with hydrogen atom of ARG60 (N----H-ARG60, 2.50 Å).

The binding interaction of 1DF7 ligand with dihydrofolate reductase active sites shows thirteen bonding interactions. The synthesized compounds bind to the enzyme in similar manner as that of 1DF7 ligand. The compounds have same H-bonding interactions with same amino acids ARG60, ARG32 and TYR100 as that of 1DF7 ligand. **Figure 10** (A and B) represents the hydrophobic and hydrophilic amino acids surrounded to the studied compound **3q** and **3w**. All the compounds showed consensus score in the range 8.73-1.57, indicating the summary of all forces of interaction between ligands and the enzyme. These scores and interactions indicate that molecules preferentially bind to the enzyme in comparison to the reference 1DF7 ligand.

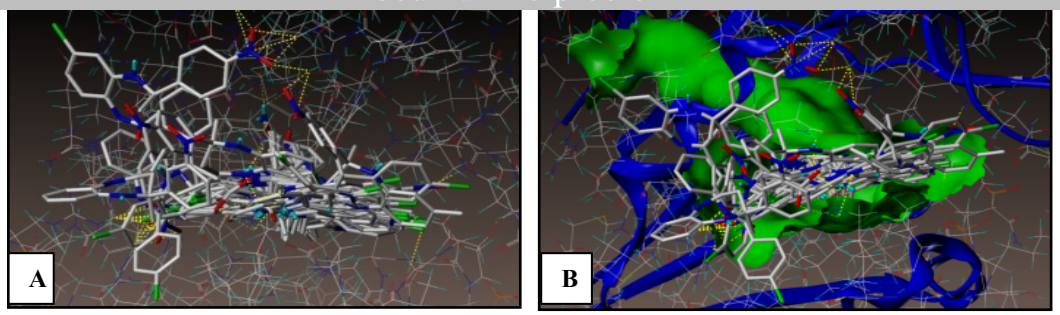

Figure 7. Docked view of all the compounds at the active site of the enzyme PDB ID: 1DF7

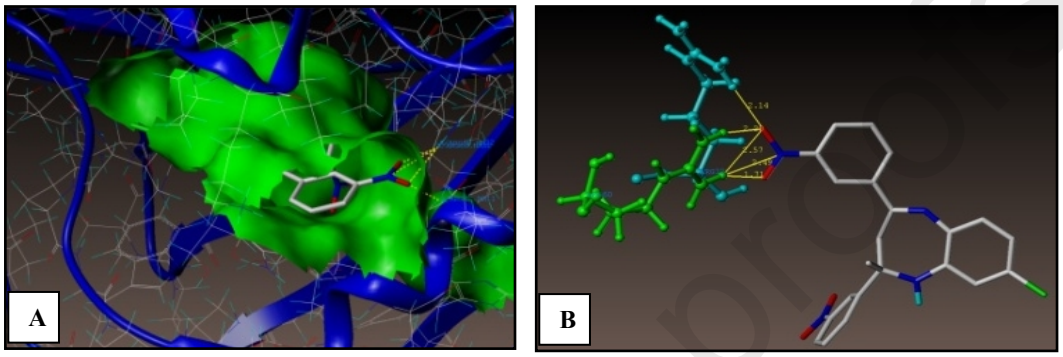

Figure 8. Docked view of compound **3q** at the active site of the enzyme PDB: 1DF7

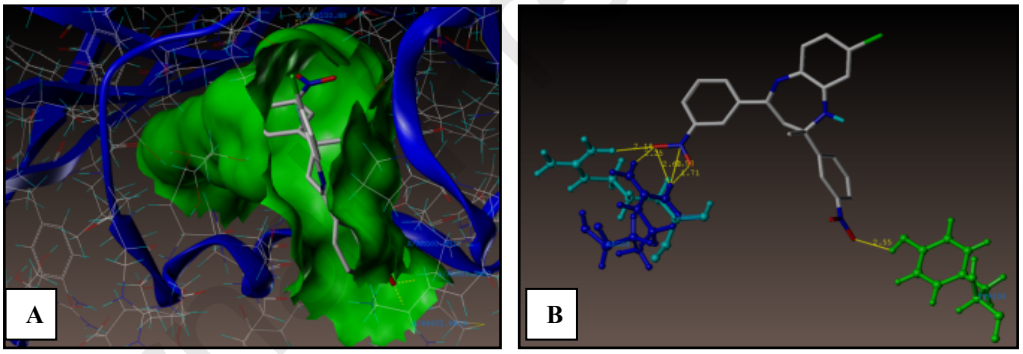

Figure 9. Docked view of compound **3w** at the active site of the enzyme PDB: 1DF7

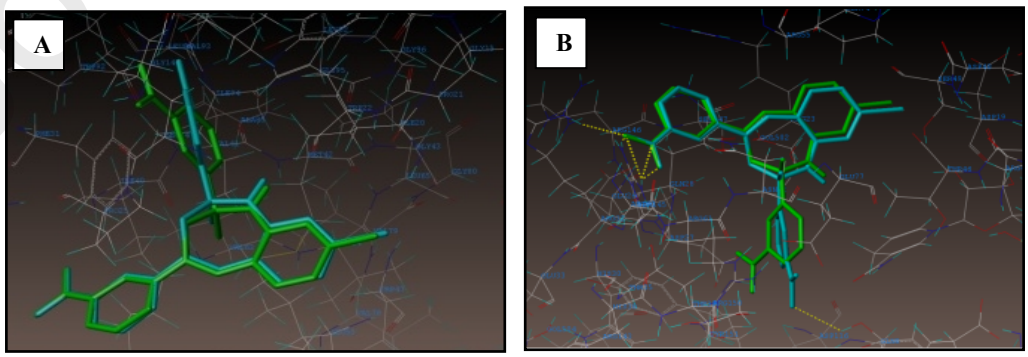

Figure 10. A) Hydrophobic amino acids surrounded to compounds **3q** (green colour) and **3w** (cyan colour) B) Hydrophilic amino acids surrounded to compounds **3q** and **3w**.

In silico molecular docking study was performed on the compounds with Molegro Virtual Docker (MVD-2007, 6.0). **Figure 11** shows the structure of EGFR-tyrosine kinase complexed with a 4-anilinoquinazoline inhibitor obtained from Protein Data Bank with the PDB ID: 1m17.

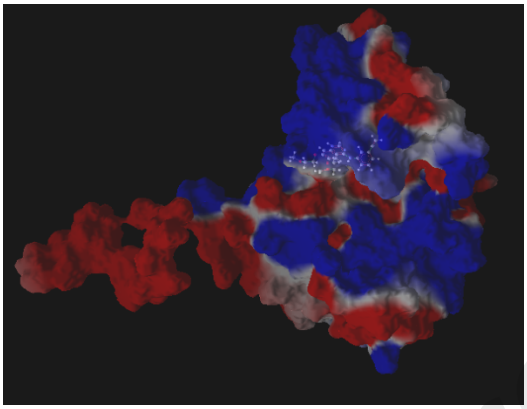

Figure 11: Structure of EGFR-tyrosine kinase domain complexed with 4-anilinoquinazoline inhibitor (PDB ID: 1m17)

The crystal structure of the target enzyme including forty amino acids from the carboxyl-terminal tail has been determined to 2.6 A resolution. Unlike any other kinase enzymes, the EGFR family members possess constitutive kinase activity without a phosphorylation event within their kinase domains. Despite its lack of phosphorylation, the EGFRK activation loop adopts a conformation similar to that of the phosphorylated active form of the kinase domain from the insulin receptor. It is observed that the key residues of a dimerized structure lying between the EGFRK domain and carboxyl terminal substrate docking sites are found in close contact with the kinase domain. The site at which the known 4-anilinoquinazoline inhibitor binds with the target protein was selected as the active site. It is lined with amino acid residues such as Leu694, Met769, Thr830, Asp831, Glu738, Lys721, Cys773; *etc*.

Hence to identify other residual interactions of the tested compounds, a grid box (include residues within a 15.0 A radius) large enough to accommodate the active site was constructed. Since 4-Anilinoquinazoline is a known inhibitor, the centre of this site was considered as the centre of search space for docking. Docking of the synthesized compounds with EGFR tyrosine kinase domain exhibited well conserved hydrogen bonding with the amino acid residues at the active site. The MolDock scores of the test compounds ranged from -86.2649 to -116.861 while that of 4-anilinoquinazoline was -127.098.

The molecular docking study revealed that compounds **3n**, **3s**, **3y** and **3x** acts as good inhibitors of tyrosine kinase due to characteristic features. However, compounds **3a-3a'** were found to be active with the target PDB ID: 1M17. The best docked poses of the compounds are depicted in **Figure 12**. Compound **3n** makes two hydrogen bond interactions at the active site of the enzyme. The interactions are raised by nitro group present on phenyl rings with Thr766 and Thr830. Compound **3z** and **3x** exhibited three hydrogen interactions

of benzodiazepine ring with Thr766.

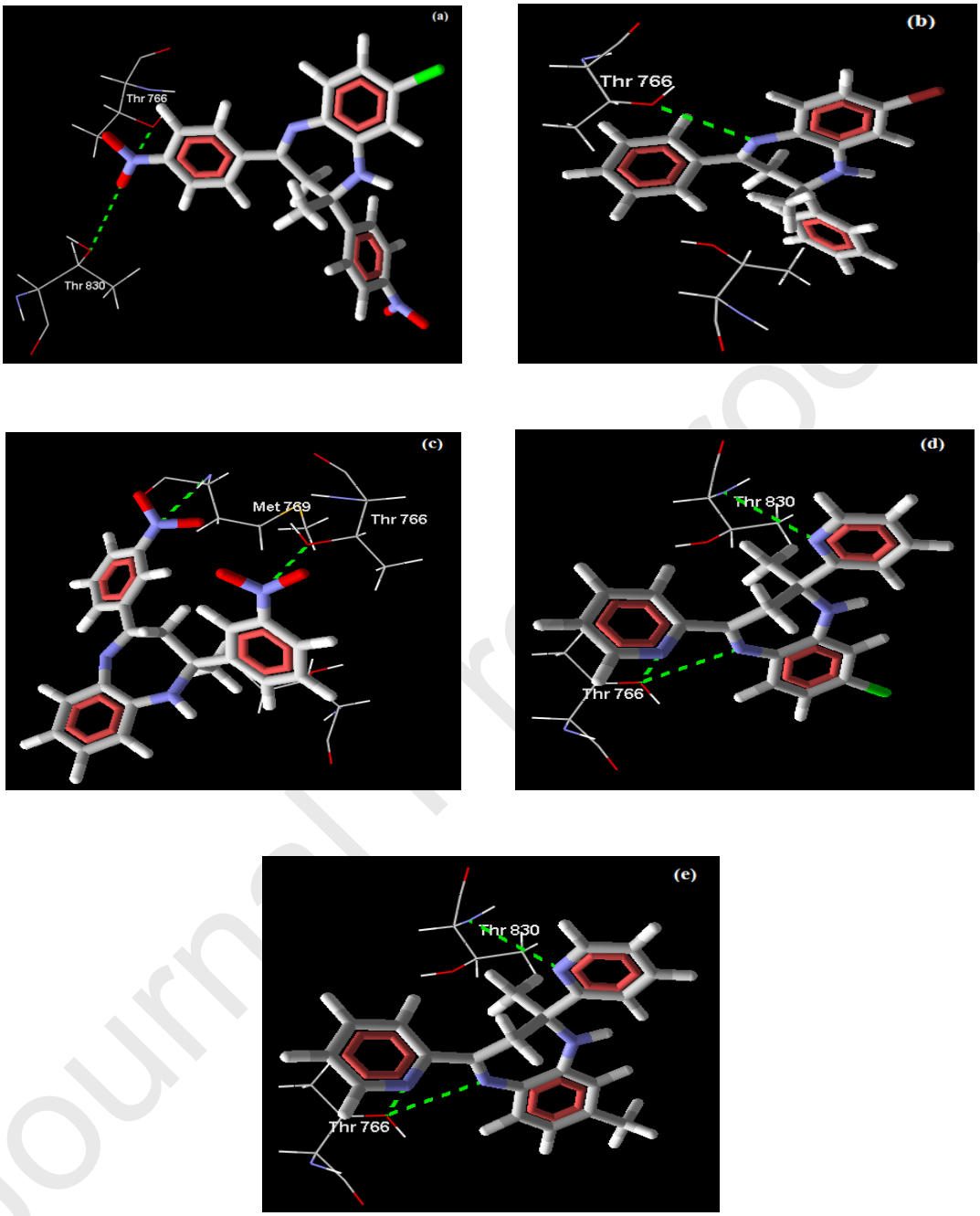

Figure 12: Molecular docking data: The compounds docked in best of its conformation into the binding site of 1M17. **a** Binding mode of compound 3l forming two H bonds with Thr766 and Thr830;**b** binding mode of compound 3n forming one H bonds with Thr766; **c** binding mode of compound 3s forming two H bonds with Met769 and Thr766; **d** & **e** binding modes of compound 4g and 4h forming two H bonds with Thr766 and Thr830, one H bond with Thr766.

2.2.3.3 Docking studies on DNA intercalation:

of interaction of drug molecule with DNA have been an interesting path towards design and development of novel highly effective drug molecules. Interaction of drug molecule with DNA leads to a sequence of operations such as structural modifications, thereby killing the unwanted cells via disrupting its replication, transcription and repair. To study the interactions of the most active benzodiazepine **3x** among the synthesized derivative and to indicate the site of interaction, primary molecular docking studies were performed.

Ligand	2K4L	
	Docking Score	MMGBSA bind
3x	-8.318	-60.49

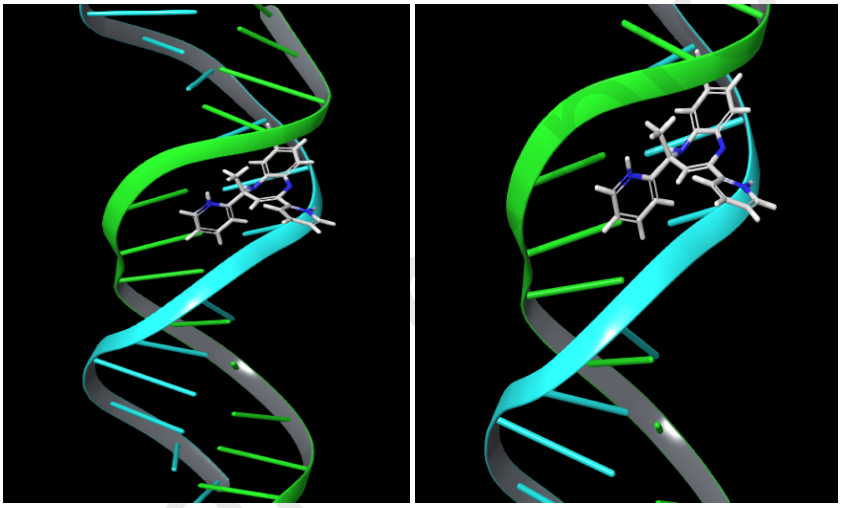

Figure 13: Docked view of compound **3x** intercalated into the DNA fragment

The molecule **3x** had high docking score of —8.3 kcal/mol. Visual inspection revealed that the ligands get intercalated in the minor grove of the DNA fragment. N^1 atom of benzodiazepine forms hydrogen bond with Thiamine while N atom of 4-pyridine ring forms hydrogen bond with adenine of the chain B of the DNA fragment. The 2-pyridine ring exhibits pi-stacked in-between two adenine rings of the DNA chain A.

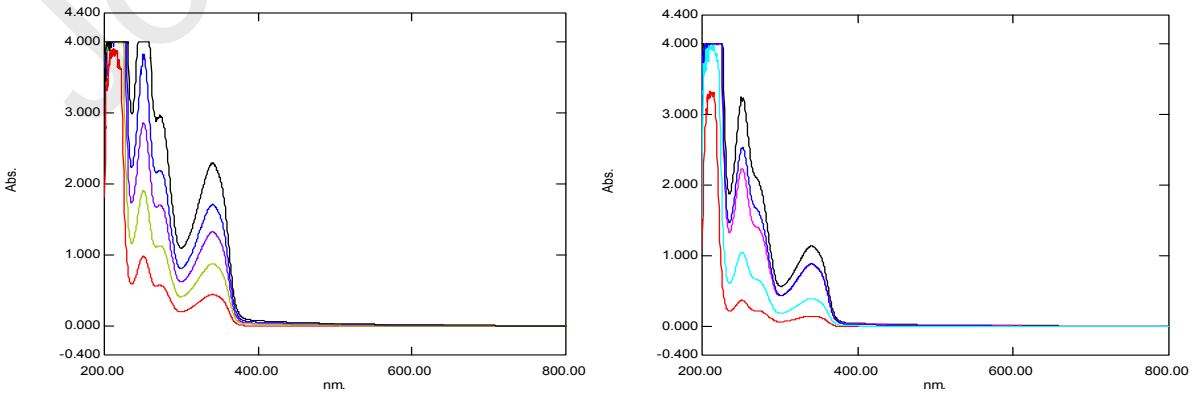

Figure 14: DNA binding studies using UV spectroscopy

For a molecule to be 'druglike', its molecular structure and biological effectiveness must be in a perfect harmony. There are various methods wherein the druglikeness can be analysed virtually considering the lipinski's RO5. In view of this, the toxicity and its feasibility to act like a drug were predicted for the synthesized compounds using Data Warrior 5.2.1. The toxicity results are presented in the following table. Based on the property calculation have favorable cLogP which should be ideally between 2.0 and 5.0 with some outliers (**3b**, **3c**, **3h**, **3i**, **3j**, **3m**, **3o**, **3p**, **3r**, **3s**, **3u**, **3y**, **3a'**). Compounds that exhibit drug likeliness based on the prediction are **3a**, **3c**, **3f**, **3l**, **3m**, **3p**, **3v**, **3x**, **3y**, **3z**, **3a'**. Most of the compounds are devoid of toxicities except **3l** and **3u** which are possibly mutagenic while **3a** and **3f** are probably teratogenic.

Table 5: Toxicity prediction using data warrior 5.2.1

Ligands	*Mutagenic*	*Tumorigenic*	*Teratogenic*	*Irritant*
3a	none	none	**high**	none
3f	none	none	**high**	none
3l	**high**	none	none	none
3u	**high**	none	none	none

Table 6: Ligands predicted with druglike properties obeying lipinski's RO5 with no toxicity parameters

Ligands	*Total Mol Weight*	*cLogP*	*H-bond Acceptors*	*H-bond Donors*	*Total Surface Area*	*Druglikeness*
3d	402.41	2.66	8	1	297.48	-3.80
3e	402.41	2.66	8	1	297.48	-3.80
3g	416.44	3.00	8	1	309.74	-3.80
3k	416.44	3.00	8	1	309.74	-3.80
3n	452.90	3.26	8	1	312.90	-3.72
3q	436.85	3.26	8	1	312.90	-3.72
3t	481.31	3.38	8	1	316.11	-5.59
3w	402.41	2.66	8	1	297.48	-3.80
3x	328.42	2.95	4	1	259.92	1.37
3z	348.84	3.11	4	1	263.08	1.43

3. Conclusion

In conclusion, we have developed an efficient and convenient catalytic method for the synthesis of new derivatives of 2-Methyl-2,4-diphenyl-2,3-dihydro-1H-benzo[1,5]diazepine under solvent free reaction conditions. The current method is advantageous due to low environmental impact, clean reaction conditions, wide substrate scope of the reaction, use of non-toxic, metal free and inexpensive catalyst which makes this procedure a green alternative to the reported tedious methods for the synthesis of 1,5-benzodiazepines. The synthesized derivatives were characterized using NMR and Mass spectroscopy. Based on the molecular docking study, the best docked compounds **3a**, **3k**, **3q**, **3w**, **3x** and **3y** were screened biologically for their anti-tumor activity studies. Significant anti-proliferative activity was demonstrated by all the assessed compounds against

human embryonic kidney) cell line. Compound **3x** was found to be the most versatile amongst all the compounds exhibiting both anti-tumor with the IC_{50} value of 0.067 ± 0.002 against HeLa cell line supported by apoptosis inducing mode of cell death. Drug synergism plays a key role in improving efficacy of drug. In order to exploit the synergistic behavior of the most potent compound **3x**, we performed synergistic activity in cytotoxicity studies of the same with drug Methotrexate. These studies were performed against HepG2 and HeLa cell lines with IC_{50} values of 0.046 ± 0.002 and 0.057 ± 0.002 which were better than the values of drug alone. Further this combination also showed promising results in apoptosis studies. The anticancer mechanistic studies indicated the compound **3x** to be good DNA intercalating agent. This proved that compound **3x** has a potency to be good lead to develop into drug molecule. DNA toxicity assessment prediction studies revealed the drug likeness of such compounds. Moreover, the present study endeavors an initiative approach for development of such targets, as good leads for enhancing the research scope for further exploitation of these molecules by broadening the efficacy of such novel molecules as potential anticancer agents.

4. Experimental

4.2. Material methods:

All commercially available solvents and reagents were purchased from SD-fine, Loba Chemie and Avra synthesis. o-phenylenediamines were used after recrystallization. Melting points were measured using open capillary tube method. The reactions were monitored by TLC carried out on Macherey – Nagel pre-coated TLC sheets SIL G/UV254 and visualized under UV light. SDFCL silica gel (200-400 mesh) was used for flash chromatography (Combi Flash Companion by Teledyne Isco). 1H and 13C NMR spectra were recorded on Bruker model 400 MHz instrument using CDCl3 solution. Chemical shifts (δ) are expressed in ppm (parts per million) relative to the residual solvent peaks as an internal standard (1H NMR: CDCl3 at 7.24 ppm, 13C NMR at 77.00 ppm) and coupling constant (J) are given in hertz. IR spectra were recorded on a Schimadzu Fourier Transform Infrared Spectrometer using KBr pallets. High resolution mass spectroscopy data were obtained in electron impact (EI) mode. Intensities are reported as percentages relative to the base peak (I= 100%).

4.3. General procedure for synthesis:

o-phenylene diamine substrate (1mmol) and substituted ketone derivative (2mmol) were taken in a round bottom flask. To that 5mol% of thiamine hydrochloride was added and heated on water bath at 70-80^{o}C for the time indicated in scheme 2. The reaction was monitored periodically till its completion. The reaction mixture was then quenched in cold water (15 mL), which was further extracted using ethyl acetate (3 x 10 mL) and dried over anhydrous Na_2SO_4. The crude product obtained was further purified using column chromatography pet ether- EtOAc (9:1). The isolated pure product was then characterized using IR, NMR and Mass spectropscopy.

4.4. Spectral data

168-170°C; IR (KBr) (ν_{max} , cm^{-1}): 3315, 1597, 1517, 1350. ^{1}HNMR(400 MHz, $CDCl_3$) (δ, ppm): 1.72 (s, 3H, CH_3- cyclic), 2.33 (s, 3H, CH_3- Ar) 2.88 (d, 1H, J= 13.2 Hz, CH_2^a), 3.08 (d, 1H, J=13.2 Hz, CH_2^b), 3.4 (s, 1H, -NH), 6.64 (d, 1H, Ar-H, J= 0.8 Hz), 6.74 (d, 1H, Ar-H, J= 8 Hz), 6.86- 6.89 (dd, 1H, Ar-H, J=1.8 Hz, J=8 Hz), 7.55-7.11 (m, 8H, Ar-H) ^{13}C NMR (75MHz, $CDCl_3$) (δ, ppm): 165.6, 155.3, 150.7, 145.6, 136.0, 135.6, 134.6, 133.2, 131.2, 131.0, 129.2, 128.0, 123.3, 118.9, 113.4, 73.2, 43.2 (CH_2), 29.2, 21.2; HRMS (ESI-TOF, $[M]^+$) : calcd for $C_{23}H_{20}N_4O_4$, 416.15; found 416.1527.

2,4-Bis-(4-bromo-phenyl)-2,8-dimethyl-2,3-dihydro-1H-benzo[b][1,5]diazepine (3h): Yellow solid, mp: 142-144°C; IR (KBr) (ν_{max} , cm^{-1}): 3323, 1601, 1510, 784. ^{1}HNMR(400 MHz, $CDCl_3$) (δ, ppm): 1.76 (s, 3H, CH_3- cyclic), 2.36 (s, 3H, CH_3- Ar) 2.90 (d, 1H, J= 13.2 Hz, CH_2^a), 3.08 (d, 1H, J=13.2 Hz, CH_2^b), 3.4 (s, 1H, -NH), 6.64 (d, 1H, Ar-H, J= 0.8 Hz), 6.74- 7.76 (m, 10H, Ar-H) ^{13}C NMR (75MHz, $CDCl_3$) (δ, ppm): 165.0, 149.5, 141.5, 137.4, 136.9, 136.8, 132.4, 130.2, 130.0, 129.5, 129.0, 128.9, 125.3, 124.3, 73.1, 43.2(CH_2), 29.8, 21.1; Mol. formula : calcd for $C_{23}H_{20}N_2Br_2$, 481.99.

2,4-Bis-(4-chloro-phenyl)-2,8-dimethyl-2,3-dihydro-1H-benzo[b][1,5]diazepine (3i): Yellow solid, mp: 156-158°C; IR (KBr) (ν_{max} , cm^{-1}): 3061, 1604, 1487, 1328, 831. ^{1}HNMR(400 MHz, $CDCl_3$) (δ, ppm): 1.56 (s, 3H, CH_3- cyclic), 1.85 (s, 3H, CH_3- Ar) 3.0 (d, 1H, J= 13.2 Hz, CH_2^a), 3.72 (d, 1H, J=13.2 Hz, CH_2^b), 3.75 (s, 1H, -NH), 6.90 -8.08 (m, 11H, Ar-H) ^{13}C NMR (75MHz, $CDCl_3$) (δ, ppm): 165.1, 145.9, 140.1, 137.9, 137.0, 136.1, 135.0, 133.2, 131.7, 129.7, 129.5, 129.3, 129.1, 128.8, 128.2, 127.3, 126,9, 121.6, 72.7, 42.9 (CH_2), 29.5, 20.5; Mol. formula: Calcd for $C_{23}H_{20}N_2Cl_2$, 394.10

2,4-Bis-(3-bromo-phenyl)-2,8-dimethyl-2,3-dihydro-1H-benzo[b][1,5]diazepine (3j): Orange solid, mp: 138-140°C; IR (KBr) (ν_{max} , cm^{-1}): 3315, 1597, 1517, 1350, 752. ^{1}HNMR(400 MHz, $CDCl_3$) (δ, ppm): 1.74 (s, 3H, CH_3- cyclic), 2.34 (s, 3H, CH_3- Ar) 2.88 (d, 1H, J= 13.2 Hz, CH_2^a), 3.07 (d, 1H, J=13.2 Hz, CH_2^b), 3.43 (s, 1H, -NH), 6.75-7.73 (m, 11H, Ar-H) ^{13}C NMR (75MHz, $CDCl_3$) (δ, ppm): 164.9, 149.5, 141.5, 137.3, 136.9, 132.4, 130.2, 129.9, 129.4, 128.9, 125.4, 124.32, 122.72, 122.41, 73.3, 43.3 (CH_2), 29.8, 21.0; HRMS (ESI-TOF, $[M]^+$) : calcd for $C_{23}H_{20}N_2Br_2$, 482.00; found 482.0059.

2,8-Dimethyl-2,4-bis-(3-nitro-phenyl)-2,3-dihydro-1H-benzo[b][1,5]diazepine (3k): Orange solid, mp: 134-136°C; IR (KBr) (ν_{max} , cm^{-1}): 3313, 1598, 1516, 1349. ^{1}HNMR(400 MHz, $CDCl_3$) (δ, ppm): 1.72 (s, 3H, CH_3- cyclic), 2.33 (s, 3H, CH_3- Ar), 2.87 (d, 1H, J= 13.2 Hz, CH_2^a), 3.08 (d, 1H, J=13.2 Hz, CH_2^b), 3.43 (s, 1H, -NH), 6.64 (d, 1H, Ar-H, J= 1.2 Hz), 6.73-7.49(m, 10H, Ar-H) ^{13}C NMR (75MHz, $CDCl_3$) (δ, ppm): 164.9, 149.5, 141.5, 137.3, 136.9, 136.8, 132.4, 130.2, 130.0, 129.8, 129.0, 129.4, 129.0, 128.9, 125.4, 124.3, 122.7, 122.41, 121.62,73.1, 43.2(CH_2), 29.8, 21.8; HRMS (ESI-TOF, $[M]^+$) : Calcd for $C_{23}H_{20}N_4O_4$, 416.15; found 416.1659.

2,4-Bis-(4-methoxy-phenyl)-2,8-dimethyl-2,3-dihydro-1H-benzo[b][1,5]diazepine (3l): Yellow solid, mp: 102-104^{o}C; IR (KBr) (ν_{max} , cm^{-1}): 3331, 1589, 1508, 1247. ^{1}HNMR(400 MHz, $CDCl_3$) (δ, ppm): 1.65 (s, 3H, CH_3- cyclic), 2.26 (s, 3H, CH_3- Ar), 2.84 (d, 1H, J= 13.2 Hz, CH_2^a), 2.98 (d, 1H, J=13.2 Hz, CH_2^b), 3.42 (s, 1H, -NH), 3.67 (s, 3H, OMe), 3.72 (s, 3H, OMe) 6.59-7.60 (m, 11H, Ar-H) ^{13}C NMR (75MHz, Mol. formula : Calcd for $C_{25}H_{26}O_2N_2$, 386.20.

8-Chloro-2-methyl-2,4-bis-(4-nitro-phenyl)-2,3-dihydro-1H-benzo[b][1,5]diazepine (3n): Orange solid, mp: 162-164^{o}C; IR (KBr) (ν_{max} , cm^{-1}): 3383, 1597, 1517, 1348, 856. ^{1}HNMR(400 MHz, $CDCl_3$) (δ, ppm): 1.77 (s, 3H, CH_3- cyclic), 2.84 (d, 1H, J= 13.76 Hz, CH_2^a), 3.02 (d, 1H, J=13.76 Hz, CH_2^b), 3.37 (s, 1H, -NH), 6.87-7.58 (m, 11H, Ar-H) ^{13}C NMR (75MHz, $CDCl_3$) (δ, ppm): 163.8, 153.5, 148.4, 147.0, 138.3, 136.7, 132.7, 131.3, 127.6, 126.7, 123.7, 123.5, 122.0, 120.4, 72.5, 43.2 (CH_2), 30.6; HRMS (ESI-TOF, $[M]^+$) : calcd for $C_{22}H_{17}N_4O_4Cl$, 436.098; found 436.1004.

2,4-Bis-(4-bromo-phenyl)-8-chloro-2-methyl-2,3-dihydro-1H-benzo[b][1,5]diazepine (3o): Brownish yellow solid, mp: 154-156^{o}C; IR (KBr) (ν_{max} , cm^{-1}): 3279, 1604, 1589, 1517, 831, 720.^{1}HNMR(400 MHz, $CDCl_3$) (δ, ppm): 1.73 (s, 3H, CH_3- cyclic), 2.85 (d, 1H, J= 18 Hz, CH_2^a), 3.11 (d, 1H, J=18 Hz, CH_2^b), 3.52 (s, 1H, -NH), 6.75-7.72 (m, 11H, Ar-H) ^{13}C NMR (75MHz, $CDCl_3$) (δ, ppm): 166.1, 145.9, 140.8, 138.7, 137.7, 136.1, 131.4, 131.3, 130.1, 129.8, 128.6, 128.5, 128.0, 127.3, 126.8, 125.0, 124.8, 122.4, 121.4, 120.61, 72.7, 43.0 (CH_2), 29.6; HRMS (ESI-TOF, $[M]^+$) : Calcd for $C_{22}H_{17}N_2Br_2Cl$, 501.95; found 501.9589.

8-Chloro-2,4-bis-(4-chloro-phenyl)-2-methyl-2,3-dihydro-1H-benzo[b][1,5]diazepine (3p): Yellow solid, mp: 146-148^{o}C; IR (KBr) (ν_{max} , cm^{-1}): 3269, 1604, 1591, 1469, 810. ^{1}HNMR(400 MHz, $CDCl_3$) (δ, ppm): 1.74 (s, 3H, CH_3- cyclic), 2.87 (d, 1H, J= 13.5 Hz, CH_2^a), 3.08 (d, 1H, J=13.5 Hz, CH_2^b), 3.51 (s, 1H, -NH), 6.73-7.50 (m, 11H, Ar-H) ^{13}C NMR (75MHz, $CDCl_3$) (δ, ppm): 166.2, 145.4, 141.0, 138.7, 137.6, 136.3, 133.3, 131.5, 130.5, 130.1, 128.5, 128.4, 128.3, 128.0, 127.0, 126.3, 122.5, 121.8, 120.7, 73.7, 43.1 (CH_2), 29.7; HRMS (ESI-TOF, $[M]^+$) : Calcd for $C_{22}H_{17}Cl_3N_2$, 414.05; found 414.0513.

8-Chloro-2-methyl-2,4-bis-(3-nitro-phenyl)-2,3-dihydro-1H-benzo[b][1,5]diazepine (3q): Orange solid, mp: 138-140^{o}C; IR (KBr) (ν_{max} , cm^{-1}): 3317, 1605, 1518, 1350. ^{1}HNMR(400 MHz, $CDCl_3$) (δ, ppm): 1.97 (s, 3H, CH_3- cyclic), 2.95 (d, 1H, J= 13.5 Hz, CH_2^a), 3.30 (d, 1H, J=13.5 Hz, CH_2^b), 3.90 (s, 1H, -NH), 6.92-8.38 (m, 11H, Ar-H) ^{13}C NMR (75MHz, $CDCl_3$) (δ, ppm): 164.1, 148.7, 148.2, 148.0, 140.4, 138.4, 137.2, 132.5, 132.2, 131.9, 130.5, 129.6, 129.3, 124.6, 122.4, 122.0, 121.6, 120.8, 120.7, 73.3, 43.1 (CH_2), 30.3; HRMS (ESI-TOF, $[M]^+$) : Calcd for $C_{23}H_{17}N_4O_4Cl$, 436.09; found 436.1004.

2,4-Bis-(3-bromo-phenyl)-8-chloro-2-methyl-2,3-dihydro-1H-benzo[b][1,5]diazepine (3r): Yellow solid, mp: 124-126°C; IR (KBr) (ν_{max} , cm^{-1}): 3277, 1605, 1581, 1487, 821, 715. ^{1}HNMR(400 MHz, $CDCl_3$) (δ, ppm): 1.71 (s, 3H, CH_3- cyclic), 2.85 (d, 1H, J= 18 Hz, CH_2^a), 3.05 (d, 1H, J=18 Hz, CH_2^b), 3.62 (s, 1H, -NH), 6.83-7.65 (m, 11H, Ar-H) ^{13}C NMR (75MHz, $CDCl_3$) (δ, ppm): 166.1, 149.0, 141.1, 138.7, 137.7, 132.8 131.6, 130.1, 129.0, 128.0, 126.8, 126.5, 125.5, 124.3, 122.8, 122.5, 121.7, 120.7, 73.2, 43.3 (CH_2), 30.1; HRMS (ESI-TOF, $[M]^+$) : Calcd for $C_{22}H_{17}N_2Br_2Cl$, 501.95; found 501.9589.

8-Chloro-2-methyl-2,4-bis-(4-fluoro-phenyl)-2,3-dihydro-1H-benzo[b][1,5]diazepine (3q): Orange solid, mp: 138-140°C; IR (KBr) (ν_{max} , cm^{-1}): 3317, 1605, 1518, 1350. ^{1}HNMR(400 MHz, $CDCl_3$) (δ, ppm): 1.73 (s, 3H, CH_3- cyclic), 2.87 (d, 1H, J= 13.5 Hz, CH_2^a), 3.09 (d, 1H, J=13.5 Hz, CH_2^b), 3.48 (s, 1H, -NH), 6.82-7.52 (m, 11H, Ar-H) ^{13}C NMR (75MHz, $CDCl_3$) (δ, ppm): 166.5, 142.6, 138.7, 138.2, 136.3, 135.4, 131.2, 129.9, 129.0, 127.4, 127.3, 126.1, 122.6, 121.8, 120.8, 115.2, 115.0, 114.8, 73.1, 43.4 (CH_2), 30.2; HRMS (ESI-TOF, $[M]^+$) : Calcd for $C_{23}H_{17}N_2F_2Cl$, 382.10; found 382.1169.

8-Bromo-2-methyl-2,4-bis-(4-nitro-phenyl)-2,3-dihydro-1H-benzo[b][1,5]diazepine (3t): Orange solid, mp: 162-164°C; IR (KBr) (ν_{max} , cm^{-1}): 3390, 1597, 1517, 1347. ^{1}HNMR(400 MHz, $CDCl_3$) (δ, ppm): 1.83 (s, 3H, CH_3- cyclic), 2.97 (d, 1H, J= 13.32 Hz, CH_2^a), 3.35 (d, 1H, J=13.32 Hz, CH_2^b), 3.72 (s, 1H, -NH), 7.04-8.06 (m, 11H, Ar-H) ^{13}C NMR (75MHz, $CDCl_3$) (δ, ppm): 166.6, 142.6, 138.8, 138.2, 136.3, 135.4, 131.2, 129.9, 129.2, 129.1, 127.4, 127.3, 126.1, 122.6, 121.8, 120.8, 115.2, 115.1, 115.0, 73.1, 43.4(CH_2), 30.1; HRMS (ESI-TOF, $[M]^+$) : calcd for $C_{22}H_{17}N_4O_4Br$, 480.042; found 480.0500.

8-Bromo-2,4-bis-(4-chloro-phenyl)-2-methyl-2,3-dihydro-1H-benzo[b][1,5]diazepine (3u): Orange solid, mp: 172-174°C; IR (KBr) (ν_{max} , cm^{-1}): 3269, 1604, 1469, 831. ^{1}HNMR(400 MHz, $CDCl_3$) (δ, ppm): 1.77 (s, 3H, CH_3- cyclic), 2.84 (d, 1H, J= 13.76 Hz, CH_2^a), 3.03 (d, 1H, J=13.76 Hz, CH_2^b), 3.37 (s, 1H, -NH), 6.93-7.58 (m, 11H, Ar-H) ^{13}C NMR (75MHz, $CDCl_3$) (δ, ppm): 166.1, 145.3, 140.9, 138.7, 137.9, 137.5, 136.5, 136.2, 133.2, 131.4, 130.1, 128.5, 128.3, 128.0, 127.0, 126.3, 122.5, 121.8, 120.6, 73.6, 43.1(CH_2), 30.0; HRMS (ESI-TOF, $[M]^+$) : calcd for $C_{22}H_{17}BrCl_2N_2$, 458.00; found 458.0038.

8-Bromo-2,4-bis-(3,4-dimethoxy-phenyl)-2-methyl-2,3-dihydro-1H-benzo[b][1,5]diazepine (3v): Yellow solid, mp: 122-124°C; IR (KBr) (ν_{max} , cm^{-1}): 3299, 1589, 1566, 1446, 1252. ^{1}HNMR(400 MHz, $CDCl_3$) (δ, ppm): 1.76 (s, 3H, CH_3- cyclic), 2.82 (d, 1H, J= 13.32 Hz, CH_2^a), 3.02 (d, 1H, J=13.32 Hz, CH_2^b), 3.37 (s, 1H, -NH), 3.65 (s, 3H, OCH_3), 3.66 (s, 3H, OCH_3), 3.79 (s, 3H, OCH_3), 3.84 (s, 3H, OCH_3), 7.48-6.62 (m, 9H, Ar-H) ^{13}C NMR (75MHz, $CDCl_3$) (δ, ppm): 167.2, 153.3, 149.0, 147.6, 147.3, 140.5, 137.3, 130.5, 127.2, 123.0, 121.2, 119.15, 114.6, 114.2, 112.5, 110.0, 109.9, 73.3, 56.1, 43.3(CH_2), 26.3; HRMS (ESI-TOF, $[M]^+$) : Calcd for $C_{26}H_{27}Br_3N_2O_4$, 510.37; found 510.3710.

8-Chloro-2-methyl-2,4-bis-(3-nitro-phenyl)-2,3-dihydro-1H-benzo[b][1,5]diazepine (3w): Orange solid, mp: 138-140°C; IR (KBr) (ν_{max} , cm^{-1}): 3319, 1604, 1519, 1348. ^{1}HNMR(400 MHz, $CDCl_3$) (δ, ppm): 1.84 (s, 3H, CH_3- cyclic), 2.94 (d, 1H, J= 13.2 Hz, CH_2^a), 3.27 (d, 1H, J=13.2 Hz, CH_2^b), 3.91 (s, 1H, -NH), 6.77-8.40 (m, 11H, Ar-H) ^{13}C NMR (75MHz, $CDCl_3$) (δ, ppm): 164.3, 148.7, 148.0, 140.4, 138.7, 136.5, 132.6, 131.9, 131.3, 130.7, 130.0, 129.6, 129.3, 124.8, 123.0, 122.4, 120.9, 73.9, 43.0(CH_2), 30.3; HRMS (ESI-TOF, $[M]^+$) : Calcd for $C_{23}H_{17}N_4O_4Br$, 480.04; found 480.0500.

2,8-Dimethyl-2,4-di-pyridin-2-yl-2,3-dihydro-1H-benzo[b][1,5]diazepine (3x): Orange solid, mp: 112-114°C; IR (KBr) (ν_{max} , cm^{-1}): 3321, 1620, 1588, 1566, 1471. ^{1}HNMR(400 MHz, $CDCl_3$) (δ, ppm): 1.73 (s, 3H, CH_3- cyclic), 2.33 (s, 3H, CH_3- Ar) 2.87 (d, 1H, J= 12.4 Hz, CH_2^a), 3.05 (d, 1H, J=12.4 Hz, CH_2^b), 3.42 (s, 1H, -NH), 6.64-7.55 (m, 11H, Ar-H) ^{13}C NMR (75MHz, $CDCl_3$) (δ, ppm): 167.2, 163.4, 163.1, 160.9, 139.4, 129.7, 129.6, 128.6, 127.5, 127.4, 123.5, 115.4, 115.3, 115.2, 115.1, 73.4, 43.0(CH_2), 29.7, HRMS (ESI-TOF, $[M]^+$) : calcd for $C_{21}H_{20}N_4$, 328.18; found 328.1821.

2,8-Dimethyl-2,4-di-naphthalen-2-yl-2,3-dihydro-1H-benzo[b][1,5]diazepine (3y): Yellow solid, mp: 138-140°C; IR (KBr) (ν_{max} , cm^{-1}): 3282, 1612, 1469,1321. ^{1}HNMR(400 MHz, $CDCl_3$) (δ, ppm): 1.87 (s, 3H, CH_3- cyclic), 2.37 (s, 3H, CH_3- Ar) 3.15 (d, 1H, J= 13.2 Hz, CH_2^a), 3.35 (d, 1H, J=13.2 Hz, CH_2^b), 3.61 (s, 1H, -NH), 6.71 (d, 1H, Ar-H, J= 0.8 Hz), 6.80 – 8.10 (m, 17H, Ar-H) ^{13}C NMR (75MHz, $CDCl_3$) (δ, ppm): 166.7, 145.0, 138.0, 137.7, 137.2, 136.9, 136.4, 135.5, 133.9, 133.8, 133.1, 132.7, 131.6, 128.7, 128.2, 127.6, 127.3, 126.8, 126.7, 126.1, 125.9, 124.3, 124.1, 124.0, 122.6, 73.3, 42.9(CH_2), 29.7, 20.6; HRMS (ESI-TOF, $[M]^+$) : calcd for $C_{31}H_{26}N_2$, 426.21; found 426.2162.

8-Chloro-2-methyl-2,4-di-pyridin-4-yl-2,3-dihydro-1H-benzo[b][1,5]diazepine (3z): Yellow solid, mp: 132-134°C; IR (KBr) (ν_{max} , cm^{-1}): 3332, 1618, 1589, 1568, 1476. ^{1}HNMR(400 MHz, $CDCl_3$) (δ, ppm): 1.87 (s, 3H, CH_3- cyclic), 3.04 (d, 1H, J= 12.4 Hz, CH_2^a), 3.30(d, 1H, J=12.4 Hz, CH_2^b), 3.68 (s, 1H, -NH), 6.84-8.45 (m, 11H, Ar-H) ^{13}C NMR (75MHz, $CDCl_3$) (δ, ppm): 166.3, 155.5, 149.0, 147.3, 145.9, 138.0, 136.0, 133.3, 126.2, 124.8, 123.4, 121.9, 121.0, 118.5, 115.5, 73.4, 43.5(CH_2), 26.3; HRMS (ESI-TOF, $[M]^+$) : Calcd for $C_{20}H_{17}N_4Cl$, 348.11; found 348.1715.

8-Chloro-2-methyl-2,4-di-naphthalen-2-yl-2,3-dihydro-1H-benzo[b][1,5]diazepine: (3a[1]): Yellow solid, mp: 168-170°C; IR (KBr) (ν_{max} , cm^{-1}): 3327, 1597, 1574, 1450, 828. ^{1}HNMR(400 MHz, $CDCl_3$) (δ, ppm): 1.87 (s, 3H, CH_3- cyclic), 3.13 (d, 1H, J= 13.2 Hz, CH_2^a), 3.44 (d, 1H, J=13.2 Hz, CH_2^b), 3.69 (s, 1H, -NH), 6.79 – 8.05 (m, 17H, Ar-H) ^{13}C NMR (75MHz, $CDCl_3$) (δ, ppm): 167.8, 144.5, 130.1, 128.4, 128.3, 127.8, 127.7, 127.5, 127.4, 127.0, 126.4, 126.2, 124.2, 124.1, 123.9, 121.8, 73.5, 43.0(CH_2), 29.9; HRMS (ESI-TOF, $[M]^+$) : calcd for $C_{30}H_{23}ClN_2$, 446.15; found 446.1523.

4.5 Tyrosine kinase *enzyme inhibition studies*

Materials: FBS (Gibco, Invitrogen) Cat No -10270106, Antibiotic – Antimycotic 100X solution (Thermofisher Scientific)-Cat No-15240062, 96-well plates**,** Universal Tyrosine Kinase Assay Kit- Cat No –MK410

Methodology

Cell Treatment:

In a 96-well flat-bottom micro plate, maintained at 37ºC in 95% humidity and 5% CO2 for overnight, the cells were seeded at a density of approximately 1×105cells/well followed by treatment with different concentration of test samples. The cells were then incubated for another 24 hours. The phosphate buffer solution, and 1 ml of extraction buffer was used to wash the cells in well for twice. The cells were then recovered carefully using cell scraper and were centrifuged at 4ºC for 10 min at 10,000 rpm. The supernatant was collected and stored for further analysis.

Tyrosine Kinase Assay:

For carrying out the assay, collected supernatant was diluted by 25 times with kinase reacting solution. The diluted control and the treated sample were added in each well in duplicate. This was followed by addition of 10 µl of 40 mM ATP-2Na solution into each well and was mixed thoroughly. Treated wells were incubated for 30 min at 37ºC. after removing the samples, wells were washed thrice with wash buffer. Next, 100µl of blocking solution was added into each well and incubated for 30 min at 37ºC. The blocking solution was then discarded and 50 µl of Anti-phosphotyrosine - HRP solution was added into each well and incubated for 30 min at 37ºC. Once the antibody solution was discared each well was washed 4 times with washing buffer followed by addition of 100 µl of HRP substrate solution (TMBZ) into each well and incubation for 30 min at 37ºC . Then 100 µl of stop solution was added into each well in the same order as HRP substrate solution and finally absorbance was measured at 450 nm with a plate reader. The percent inhibition was calculated using the below formula

% Inhibition = 1- (Abs of sample /Abs of control) x 100

The $IC_{50}$of compounds was calculated using graph Pad Prism Version5.1 by taking a percentage of Inhibition Tyrosine Kinase Enzyme at six different concentrations of treatment.

4.6 Cytotoxicity assay:

The in-vitro cytotoxicity studies of selective compounds **3a**, **3k**, **3q**, **3w**, **3y** and **3x** was assessed by MTT assay [65] using three different cell lines namely HeLa, HEPG2 and HEK-293. Cytotoxicity studies were also evaluated against Paclitaxel and Methotrexate as standard drugs. Firstly, the cell lines were seeded in 96 well flat-bottom micro plate containing Dulbecco's Modified Eagle Media (DMEM) supplemented with 10% heat inactivated fetal bovine serum and 1% antibiotic- antimycotic 100X solution. The cells were maintained overnight at 37ºC in 95% humidity & 5% CO2 and were seeded in separate 96 well plates. The compound

addition of MTT solution. The wells were washed with phosphate buffer solution two times followed by addition of 20 µL of MTT solution and then incubated at 37°C. After 4h, formazan crystals were dissolved using 100 µL DMSO and absorbance was recorded at 570 nm using microplate reader. The IC_{50} calculation was carried out using graph pad prism version 5.1.

4.7 Apoptosis studies using flowcytometry:

Materials: Cell lines – Hep G2 (Liver cancer), DMEM with low glucose (Cat No-11875-093), FBS (Gibco, Invitrogen) Cat No -10270106, Antibiotic – Antimycotic 100X solution (Thermofisher Scientific)-Cat No-15240062, AnnexinV-FITC Kit (Beckman Coulter) Cat No –PN IM 3546- 200 Tests, Propedium Idiode (Sigma-Aldrich) Cat No –P 4170

Methodology:

A 24-well flat bottom micro plate containing cover slips, maintained at 37^0C in CO_2 incubator for overnight was used for seeding the cells. The cells were treated with 20µg/ml of each sample compound at 24 hrs. After incubation, cells were then washed with PBS and Centrifuged for 5 minutes at 500 x g at 4°C. Supernatant was discarded, and the cell pellets were resuspended in ice-cold 1X Binding Buffer to 1 x105 per mL. The tubes were kept on ice and 1 µL of annexin V-FITC solution and 5 µL PI was added. It was mixed gently and incubated for 15 minutes in the dark. Followed by this, 400 µL of ice-cold 1X binding buffer was added and mixed gently. The cell preparations were then analyzed by flowcytometry within 30 minutes.

4.8 Molecular docking:

4.8.1 As DHFR target

Molecular docking was used to clarify the binding mode of the compounds to provide straightforward information for further structural optimization. The crystal structure of dihydrofolate reductase complexed with NADPH and Methotrexate (PDB ID 1DF7, 1.7 Å X-ray resolutions) was extracted from the Brookhaven Protein Database (PDB http://www.rcsb.org/pdb). The proteins were prepared for docking by adding polar hydrogen atom with Gasteiger-Huckel charges and water molecules were removed. The 3D structure of the ligands was generated by the SKETCH module implemented in the SYBYL program (Tripos Inc., St. Louis, USA) and its energy-minimized conformation was obtained with the help of the Tripos force field using Gasteiger-Huckel charges and molecular docking was performed with Surflex-Dock program that is interfaced with Sybyl-X 2.0. and other miscellaneous parameters were assigned with the default values given by the softwa*re*

4.8.2 As anticancer target

Ligand Preparation

The molecules **3b**, **3w** and **3x** were prepared using *LigPrep* module in the *Schrodinger Suite 2018-4* (Trial Version). The stereoisomerism of the chiral centers in the molecules synthesized was racemic, hence all the stereoisomers were generated for the purpose of docking. The molecules were neutral as a results ionization

used for docking studies.

Docking

The active ligands were docked into the receptor grid generated around the inhibitor bound to the protein crystal structure. The outer grid 15 Å inx, y, and z extents while the inner grid was 10 Å in extents. To maximize the probability of forming hydrogen bonds between the residues in the enzyme active site and the ligand, the side chain hydroxyl groups of the amino acids serine, threonine, and tyrosine were allowed to rotate. All the calculations were carried with Schrödinger Suite 2018-4 (Trial Edition) running on Linux Workstation.

DNA binding studies:

Methodology: UV Absorption experiments were performed by maintaining a constant nucleotide concentration and varying samples concentration (10–2 μg/ml) in buffer. Solutions of calf thymus DNA in phosphate buffer gave a ratio of UV absorbance at 260 and 280 nm (A260/A280) 1.8–1.9, indicating that the DNA was pure and sufficiently free of contaminants like the proteins and RNA. The solution of DNA and desired compounds were kept to equilibrate at 25 °C for 20 min, after which absorption readings were noted. The data were then fit to following equation (1) to obtain intrinsic binding constant Kb.

$$[DNA]/ [\in_a - \in_f] = [DNA] / [\in_b - \in_f] + 1 / Kb[\in_b - \in_f] \text{ - - - } (1)$$

Where, [DNA] = concentration of DNA in base pairs,

$\in_a$ is the extinction coefficient observed for the MLCT absorption band at the given DNA concentration,

$\in_f$ is the extinction coefficient of the complex without DNA

$\in_b$ is the extinction coefficient of the complex when fully bound to DNA.

5. Acknowledgments

The authors are grateful to the Department of Science and Technology of Goa and UGC- New Delhi, DST-FIST New Delhi for financial support. We would also like to thank Department of Chemistry, Goa University for providing 1H NMR and ^{13}C NMR data, Sophisticated analytical instrument facilities, Chandigarh and Karnatak University, Dharwad, for ^{1}H NMR and ^{13}C NMR data, IIT Ropar and Birla Institute of Technology, Pilani, Rajasthan, for Mass spectral data.

6. References

Evaluation of Anticancer Activity of Nanoresveratrol in B16 Melanoma Cell Line, *Critical Reviews in Food Science and Nutrition*, **2017**, *58(9)*, 1428.

2. Cook S; Salmon P; Hayes G; Byrne A; Fisher P, Predictors of emotional distress a year or more after diagnosis of cancer: A systematic review of the literature*, Psycho-Oncology,* **2018***, 27(3),* 791.
3. Youn Y; Bae Y, Perspectives on the past, present, and future of cancer nanomedicine*, Advanced Drug Delivery Reviews,* **2018,** *130*, 3.
4. Bayat R; Homayouni T; Baluch N; Morgatskaya E; Kumar S; Das B, Combination therapy in combating cancer, *Oncotarget*, **2017**, *8*, 38022.
5. Palmer A; Sorger P, Combination cancer therapy can confer benefit via patient-to-patient variability without drug additivity or synergy, *Cell*, **2017**, *171*, 1678.
6. Narayan R; Molenaar P; Teng J; Cornelissen F; Roelofs I; Menezes R; Dik R; Lagerweij T; Broersma A; Petersen N; Soto J; Brands E; Kuiken P; Lecca M; Lenos K; Veld S; Wieringen W; Lang F; Sulman E; Verhaak R; Baumert B; Stalpers L; Vermeulen L; WattsC; Bailey D; Slotman B; Versteeg R; Noske D; Sminia P; Tannous B; Wurdinger T; Koster J; Westerma B, A cancer drug atlas enables synergistic targeting of independent drug vulnerabilities, *Nature Communications*, **2020**, *11*, 2935.
7. Sugahara K; Teesalu T; Karmali P; Kotamraju V; Agemy L; Greenwald D, Coadministration of a tumor-penetrating peptide enhances the efficacy of cancer drugs, *Science*, **2020**, *328*, 1031.
8. Holohan C; Van Schaeybroeck S; Longley D; Johnston P, Cancer drug resistance: an evolving paradigm, *Nature Reviews Cancer*, **2013**, *13*, 714.
9. Crystal, A. S., Shaw, A. T., Sequist, L. V., Friboulet, L., Niederst, M. J., Lockerman, E. L., et al. (2014). Patient-derived models of acquired resistance can identify effective drug combinations for cancer. Science 346, 1480–1486. doi: 10.1126/science.1254721.
10. Paul M; Mukhopadhyay A, Tyrosine kinase – Role and significance in Cancer, *Int. J. Med. Sci.*, **2004**, *1*,101.
11. 8. Yamaoka T; Kusumoto S; Ando K; Ohba A; Ohmori T, Receptor Tyrosine Kinase-Targeted Cancer Therapy, *Int. J. Med. Sci.* **2018**, *19*, 3491.
12. Charles Pottier, Margaux Fresnais, Marie Gilon, Guy Jérusalem , Rémi Longuespée ,and Nor Eddine Sounni, Review: Tyrosine Kinase Inhibitors in Cancer: Breakthrough and Challenges of Targeted Therapy. Cancers **2020**, 12, 731, 1-17.
13. Yuan X; Yang Q; Liu T; Li K; Liu Y; Zhu C; Zhang Z; Li L; Zhang C; Xie M; Lin J; Zhang J; Yi Jin,Design, synthesis and in vitro evaluation of 6-amide-2-aryl benzoxazole/benzimidazole

Chemistry, **2019**, *179*, 147.

14. 10. Hossam M; Lasheen D; Ismail N; Esmat A; Mansour A; Singab A; Abouzida K, Discovery of anilinofuro[2,3-d]pyrimidine derivatives as dual inhibitors of EGFR/HER2 tyrosine kinase and their anticancer activity, *European Journal of Medicinal Chemistry*, **2018,** *144*, 330.
15. Rawluk J; Waller C, Gefitinib, *Small Molecules in Oncology*, **2018**, 235.
16. Tanaka A; Nishikawa H; Noguchi S; Sugiyama D; Morikawa H; Takeuchi Y; Ha D; Kitawaki T; Maeda Y; Saito T; Shinohara Y; Kameoka Y; Iwaisako K; Monma F; Ohishi K; Karbach J; Jager E; Sawada K; Katayama N; Takahashi N; Sakaguchi S, Tyrosine kinase inhibitor imatinib augments tumor immunity by depleting effector regulatory T cells, *The Journal of Experimental Medicine*, **2019,** *217*, 1.
17. Gold K; Kies M; William W; Johnson F; Lee J; Glisson **,** Erlotinib in the treatment of recurrent or metastatic cutaneous squamous cell carcinoma: A single-arm phase 2 clinical trial. *Cancer*, **2018**, *124*, 2169.
18. D'Amore C; Borgo C; Sarno S; Salvi M, Role of CK2 inhibitor CX-4945 in anti-cancer combination therapy – potential clinical relevance, *Cellular Oncology*, **2020**, *43*, 1003.
19. Yang Z; Tam K, Anti-cancer synergy of dichloroacetate and EGFR tyrosine kinase inhibitors in NSCLC cell lines, *European Journal of Pharmacology*, **2016**,*789*, 458.
20. Yang Z; Hu X; Zhang S; Zhang W; Tam K, Pharmacological synergism of 2,2-dichloroacetophenone and EGFR-TKi to overcome TKi-induced resistance in NSCLC cells. *European Journal of Pharmacology*, **2017**, *815*, 80.
21. Wen W; Han E; Dellinger T; Lu L; Wu J; Jove R; Yim J, Synergistic Anti-Tumor Activity by Targeting Multiple Signaling Pathways in Ovarian Cancer, Cancers, **2020**, 12, 2586.
22. Sidorov P; Naulaerts S; Ariey-Bonnet J; Pasquier E; Ballester P, Predicting Synergism of Cancer Drug Combinations Using NCI-ALMANAC Data, *Frontiers in Chemistry*, **2019**, *7*, 509.
23. Manohar S; Leung N, Cis-platin nephrotoxicity: A review of the literature, *Journal of Nephrology*, **2018**, *31*,15.
24. Yang C; Horwitz S, Taxol: The first microtubule stabilizing agent, *Int. J. Mol. Sci.*, **2017**, *18*, 1733.
25. Fawal M; Jungas T; Davy A, Inhibition of DHFR targets the self-renewing potential of brain tumor initiating cells, *Cancer Letters*, **2021**, *503*, 129.
26. Raimondi M; Randazzo O; Franca M; Barone G; Vignoni E; Rossi D; Collina S, DHFR Inhibitors: Reading the Past for Discovering Novel Anticancer Agents, **2019**, *24(6)*, 1140.
27. Saporito F; Menter M, Methotrexate and psoriasis in the era of new biologic agents, *Journal of American Academy of Dermatology,* **2004**, *50*,301.

Journal of Rheumatolog, **1997**, *36*, 1196.

29. Fernandes D; Bertino J, 5-fluorouracil-methotrexate synergy: enhancement of 5-fluorodeoxyridylate binding to thymidylate synthase by dihydropteroylpolyglutamates, Proceedings of the National Academy of Sciences, **1980**, *77*, 5663.
30. Brande J; Peppelenbosch M; Hommes D, Synergistic effect of methotrexate and infliximab on activated lymphocyte apoptosis, *Inflammatory Bowel Diseases*, **2007**, *13*, 118.
31. Akutsu M; Furukawa Y; Tsunoda S; Izumi T; Ohmine K; Kano Y, Schedule-dependent synergism and antagonism between methotrexate and cytarabine against human leukemia cell lines *in vitro*, *Leukemia*, **2002**, *16*, 1808.
32. Tietz E; Rosenberg H; Chiu T, A comparison of the anticonvulsant effects of 1, 4-and 1, 5-benzodiazepines in the amygdala-kindled rat and their effects on motor function, *Epilepsy Res.* **1989**, *3*, 31.
33. Guo F; Wu S; Julander J; Ma J; Zhang X; Kulp J; Cuconati A; Block T; Du Y; Guo J; Changa J, A Novel Benzodiazepine Compound Inhibits Yellow Fever Virus Infection by Specifically Targeting NS4B Protein, *Journal of Virology*, **2016**, *90*, 10774.
34. An Y; Hao Z; Zhang X; Wang L, Efficient Synthesis and Biological Evaluation of a Novel Series of 1,5-Benzodiazepine Derivatives as Potential Antimicrobial Agents, *Chem. Biol. Drug Des*. **2016**, *88*, 110.
35. Wang L; Li X; An Y, 1, 5-Benzodiazepine derivatives as potential antimicrobial agents: design, synthesis, biological evaluation, and structure–activity relationships, ***Org. Biomol. Chem.*** **2015**, **13**, 5497.
36. Braccio M ; Grossi G; Roma G, Vargiu L; Mura M; Marongiu M, 1,5-Benzodiazepines. Part XII. Synthesis and biological evaluation of tricyclic and tetracyclic 1,5-benzodiazepine derivatives as nevirapine analogues, *Eur. J. Med. Chem.* **2001**, *36*, 935.
37. Gill R; Kaushika S; Chugh J; Bansal S; Shah A; Bariwal J, Recent Development in [1,4]Benzodiazepines as Potent Anticancer Agents: A Review *Mini-Reviews in Medicinal Chemistry*, **2014**, *14*, 229.
38. Singh R; Prasad D; Bhardwaj T, Design, synthesis and in vitro cytotoxicity study of benzodiazepine-mustard conjugates as potential brain anticancer agents, *Journal of Saudi Chemical Society*, **2017**, *21*, S86.
39. Salve P; Mali D, 1, 5-Benzodiazepine: A versatile pharmacophore, *Int. J. Pharm. Bio. Sci.* **2013**, *4*, 345.
40. Escobar C; Tauda ; Maturana R; Sicker D, Synthesis of 1, 5-benzodiazepines with unusual substitution pattern from chalcones under solvent-free microwave irradiation conditions, *Syn. Comm*. **2008**, *39*, 166.
41. Feng S, Fan X.; Shen Q., An Efficient Synthesis of 1,5-Benzodiazepine Derivatives by Lanthanide Trichloride-catalyzed Condensation of o-Phenylenediamine with α,β-Unsaturated Ketone under Mild Conditions, *Chin. J. Chem*. **2008**, *26*, 1163.
42. Wu J; Xu F; Zhou Z; Shen Q, Efficient Synthesis of 1,5-Benzodiazepine Derivatives by Ytterbium Trichloride–Catalyzed Condensation of o-Phenylenediamine and Ketones, *Syn. Comm.*, **2006**, *36*, 457.
43. Okuma K; Tanabe Y; Itoyama R; Nagahora N; Shioji K; One-pot Synthesis of 2, 3-Benzodiazepines from Arynes and β-Diketones, *Chem. Lett*. **2013**, *42*, 1260.

and antituberculosis activity of some new pyrazole, isoxazole, pyrimidine and benzodiazepine derivatives containing thiochromeno and benzothiepino moieties, *RSC Adv.*, **2013**,*3*, 19300.

45. Yang Z; Ding Z; Chen F; He Y; Yang N; Fan Q, Asymmetric Hydrogenation of Cyclic Imines of Benzoazepines and Benzodiazepines with Chiral, Cationic Ruthenium–Diamine Catalysts, *Eur. J. Org. Chem.*, **2017**, *2017*, 1973.
46. Weers M; Lühning L; Lührs V; Brahms C; Doye S, One-Pot Procedure for the Synthesis of 1,5-Benzodiazepines from N-Allyl-2-bromoanilines, *Chem. Eur. J.,* **2017**, *23*, 1237.
47. Cacchi S; Fabrizi G; Goggiamani A; Iazzetti A, Construction of the 1,5-Benzodiazepine Skeleton from o-Phenylendiamine and Propargylic Alcohols via a Domino Gold-Catalyzed Hydroamination/Cyclization Process, *Org. Lett*. **2016**, *18*, 3511.
48. Chari M; Syamasundar K; Titanium-Catalyzed Hydroaminoalkylation of Vinylsilanes and a One-Pot Procedure for the Synthesis of 1,4-Benzoazasilines, *Cat. Comm*. **2005**, *6*, 67.
49. An Y; Li X; An X; Wang L, FeCl3–SiO2 promoted one-pot, three-component synthesis of novel 1,5-benzodiazepine derivatives, *Monatsh Chem.*, **2015**, *146*, 165.
50. M. GodinoL; Diez M; Matos I; Valle C; Bernardo M; Fonseca I; Mayoral E, Enhanced Catalytic Properties of Carbon supported Zirconia and Sulfated Zirconia for the Green Synthesis of Benzodiazepines, *Chem Cat Chem*, **2018**, *10*, 5215.
51. Alinezhad H; Tajbakhsh M; Norouzi M; Bagher S, An Efficient and Green Protocol for the Synthesis of 1,5-benzodiazepine and Quinoxaline Derivatives Using Protic Pyridinium Ionic Liquid as a Catalyst, *World Applied Sciences Journal*, **2013**, 22, 1711.
52. Korbekandi M; Esfahani M; Baltork I; Moghadam M; Tangestaninejad S; Mirkhani V, Preparation and Application of a New Supported Nicotine-Based Organocatalyst for Synthesis of Various 1, 5-Benzodiazepines, *Cat. Lett*. **2019**, *149*, 1057.
53. Pasha M; Jayashankara V, An expeditious synthesis of 1, 5-benzodiazepine derivatives catalysed by p-toluenesulfonic acid, *Journal of Pharmacolgy and Toxicolgy*, **2006**, *1*, 576.
54. Baseer M; khan A, Citric Acid-catalyzed Solvent Free, an Efficient One-pot Synthesis of 2, 3-Dihydro-1H-1, 5-Benzodiazepine Derivatives, *Recent Research in Science and Technology* **2011**, *3*, 101.
55. Sivamurugan V; Deepa K; Palanichamy M; Murugesan V, [(L)Proline]2Zn Catalysed Synthesis of 1,5-Benzodiazepine Derivatives Under Solvent-Free Condition, *Syn. Comm.* **2004**, *34*, 3833.
56. Yin L; Wang L, Chemo-/regio-selective synthesis of 2-aryl-3-acetyl-2, 4-dihydro-1H-5H-1, 5-benzodiazepines using Lewis acid, CeCl3· 7H2O*, Tet. Lett.* **2016**, *57*, 5935.
57. Majee A; Sarkar A; Santra S; Kundu S; Hajra A; ZyryanovG; Chupakhin O; Charushin V, A decade update on solvent and catalyst-free neat organic reactions: a step forward towards sustainability, *Green Chem*., **2016**, *18*, 4475.
58. Pawar O; Chavan F; Suryawanshi V; Shinde V; Shinde N, Thiamine hydrochloride: An efficient catalyst for one-pot synthesis of quinoxaline derivatives at ambient temperature, *J. Chem. Sci.* **2013**, *125*, 159.

synthesis of 4H-benzo[b]pyrans in aqueous ethanol, *Res. Chem. Intermed.* **2017**, 4*3*, 3883.

60. Lei M; Ma L; Hu L, Thiamine hydrochloride as a efficient catalyst for the synthesis of amidoalkyl naphthols, *Tet. Lett.* **2009,** *50*, 6393.
61. Lei M; Ma L; Hu L, Thiamine Hydrochloride–Catalyzed One-Pot Synthesis of 1, 4-Dihydropyridine Derivatives Under Solvent-Free Conditions, *Syn. Comm.* **2011**, *41*, 1969.
62. Altaf A; Shahzad A; Gul Z; Rasool N; Badshah A; Lal B; Khan E, A Review on the medicinal importance of pyridine derivatives, *Journal of Drug Design and Medicinal Chemistry*, **2015**, *1*, 1.
63. Abozeid M; El-Sawi A; Abdelmoteleb M; Awad H; Abdel-Aziz M; Hassan Abdel-Rahman A; Ibrahim El-Desoky E, Synthesis of novel naphthalene-heterocycle hybrids with potent antitumor, anti-inflammatory and antituberculosis activities, *RSC Advances*, **2020**, *10*, 42998.
64. Wang G; Liu W; Peng Z; Huang Y; Gong Z; Li Y, Design, synthesis, molecular modeling, and biological evaluation of pyrazole-naphthalene derivatives as potential anticancer agents on MCF-7 breast cancer cells by inhibiting tubulin polymerization, *Bioorganic Chemistry*, **2020**, *103*, 104141.
65. Bhat S; Revankar V; Kumbar V; Bhat K; Kawade V, Synthesis, crystal, structure and biological properties of a cis-dichloridobis(diimine)copper(II) complex, *Acta Cryst*., **2018**, C74.
66. Pitarch A; Lopez B; Nacher A; Merino V; Sanjuan M, Impact of undernutrition on the pharmacokinetics and pharmacodynamics of anticancer drugs: A literature review, *Nutrition and Cancer*, **2017**, *69*, 1.

Highlights

- A bio-catalysed green synthesis of new 1,5-benzodiazepine derivatives have been developed.
- *In vitro* protein tyrosine kinase inhibitory activity is exhibited by selected compounds.
- *In vitro* anticancer activity and apoptotic mode of cell death have been studied.
- Pronounced synergistic anticancer potential of compound **3x** with drug Methotrexate have been showcased.
- *In silico molecular docking and* DNA binding studies of selected proved promising DNA intercalating ability.

Declaration of interests

✓ The authors declare that they have no known competing financial interests or personal relationships that could have appeared to influence the work reported in this paper.

☐The authors declare the following financial interests/personal relationships which may be considered as potential competing interests:

The manuscript work has been provisionally filed for Indian patent in January 2021.